Journal of CO2 Utilization 84 (2024) 102860

Contents lists available at ScienceDirect

Journal of CO2 Utilization

journal homepage: www.elsevier.com/locate/jcou

Research status of building materials utilization and CO_2 curing technology on typical coal-based solid waste: A critical review

Yingjie Zou [a], Qiang Song [a,b,c,*], Peng Zhang [a], Shipeng Xu [a], Jiuwen Bao [a], Shanbin Xue [a], Ling Qin [a], Hui Wang [d], Liang Lin [e], Changsha Liu [f]

[a] Center for Durability & Sustainability Studies of Shandong Province, Qingdao University of Technology, Qingdao 266033, PR China
[b] Key Laboratory of Coal Resources Exploration and Comprehensive Utilization, Ministry of Natural ResourcesXi'an 710000, PR China
[c] State Key Laboratory of Coal Resources in Western China, Xi'an University of Science and Technology, Xi'an 710000, PR China
[d] Ningbo Key Laboratory of Energy Geostructure, Ningbo 315211, PR China
[e] Qingdao West Coast New Area Ronghe Holding Group Co., Ltd, Qingdao 266400, PR China
[f] China Construction Industrial & Energy Engineering Group Co., Ltd., Jinan 250014, PR China

ARTICLE INFO

Keywords:
Coal-based solid waste
Building materials
CO_2 curing technology

ABSTRACT

Coal, one of China's most abundant natural resources, plays a crucial role in providing substantial energy and promoting economic growth. However, the disposal and storage of large quantities of coal-based solid waste (CBSW), such as coal gangue (CG), fly ash (FA), and coal gasification slag (CGS), generated during coal production and utilization processes, pose serious social and environmental challenges. The application of solid waste in the construction materials field has garnered significant attention and is anticipated to become a primary treatment method in the future. This paper comprehensively reviews the characteristics, pretreatment methods, and utilization performance of typical CBSWs, aiming to offer a basis and valuable reference for optimizing the inherent properties of solid waste and its utilization. Additionally, it discusses the influence of various carbonation curing parameters on CO_2 capture and elucidates the impact mechanism of carbonation curing on the performance of CBSW concrete. This study holds great significance for the utilization of CBSW in building materials and carbon reduction, particularly in regions with substantial solid waste and high CO_2 emissions.

1. Introduction

Coal is a crucial energy source globally, particularly for countries such as China, India, Russia, the United States, Indonesia, and Australia. Coal accounts for approximately 30 % of global energy consumption and supplies about 40 % of the world's electricity generation [1]. China is the largest coal consumer due to its resource structure, which is rich in coal but has limited natural gas and oil [2]. In 2017, China contributed to more than 50 % of the world's total coal consumption, amounting to about 8 billion tons [3]. Coal production generates 500–800 million tons of coal gangue (CG) annually during mining and washing processes; however, over 25–50 % of the CG is not recycled [4]. Additionally, various other coal-derived solid wastes (CBSW), including fly ash (FA), coal bottom ash (CBA), flue gas desulfurization gypsum (FGD), and coal gasification slag (CGS), are generated during coal utilization.

Typical coal-based solid waste, such as coal gangue (CG), significantly impacts the ecological environment. Currently, CG is disposed of through spreading and landfilling, practices considered unsustainable due to the pollution risks they pose to soil, groundwater, geology, and the atmosphere (Fig. 1) [5]. Heavy metals in CG, including Pb, Cu, Cr, Zn, As, and Mn, are particularly concerning as they are non-biodegradable and can adversely affect soil [6]. Although these heavy metals generally present a low immediate risk to local ecology, their migration from CG to soils is facilitated by the strong adsorption of colloids in the soil [7]. Over time, this migration leads to the bioaccumulation of heavy metals in crops, animals, and fish, ultimately impacting human health through the food chain. Additionally, CG contaminates surrounding groundwater, increasing the levels of polycyclic aromatic hydrocarbons (PAHs), SO_4^{2-}, and heavy metals in water [8,9]. Furthermore, the spontaneous combustion and dust pollution of CG release SO2, H2S, and NOx, contributing to fog, haze, and acid rain [10,11].

* Corresponding author at: Center for Durability & Sustainability Studies of Shandong Province, Qingdao University of Technology, Qingdao 266033, PR China.
E-mail address: songqiang3709@163.com (Q. Song).

https://doi.org/10.1016/j.jcou.2024.102860
Received 11 May 2024; Received in revised form 18 June 2024; Accepted 26 June 2024
Available online 2 July 2024

With the increasing demand for resources and environmental protection [12], the utilization of coal-based solid waste (CBSW) has significantly expanded, given its composition and characteristics. Researchers are actively developing various applications, notably in landfill [13,14], the energy industry [15,16], building materials [17–19], agriculture [20,21], and other chemical materials [22] (Fig. 2). Among CBSW, coal gangue (CG) is the most prevalent, with CG-based building materials comprising about 32 % of total CG utilization [23]. Waste building materials are increasingly attracting attention and hold promise as a primary disposal method in the future. To illustrate the influence of typical CBSW on the properties of building materials, this paper provides a comprehensive review of the composition, pretreatment, and utilization performance of CBSW in building materials. Additionally, the paper discusses the CO_2 capture potential of CBSW building materials in response to the global demand for carbon reduction. This review aims to share valuable information with researchers in environmental science, building materials, the chemical industry, and energy. The utilization of CBSW in building materials and its CO_2 capture potential can significantly contribute to recycling solid waste, especially in regions with substantial solid waste and high CO_2 emissions.

2. Properties of various CBSW

2.1. CG

Coal gangue (CG) represents the largest stockpile of coal-based solid waste (CBSW), with fly ash (FA) production volume slightly lower. Together, CG and FA constitute approximately 80 % of the total CBSW. Typically, CG is gray and fissile, and it can be considered a mixture of inorganic materials (claystone, sandstone, carbonate rock, aluminous rock, etc.), organic elements (C, H, O, N, S), and trace elements (e.g., gallium, vanadium, titanium, cobalt) [24]. The main chemical components of CG are SiO_2, Al_2O_3, Fe_2O_3, CaO, MgO, K_2O, and SO_3. A summary of eleven CG samples reveals that SiO_2 and Al_2O_3 account for about 80 % of all compositions, with SiO_2 and Al_2O_3 contents ranging from 38.85 % to 65.87 % and 17.35–32.80 %, respectively [25–31] (Fig. 3a). The chemical composition reflects its mineral composition; for instance, the presence of SiO_2, Al_2O_3, K_2O, and Na_2O indicates quartz, kaolinite, mica, and feldspar. CaO, MgO, and Fe_2O_3 are associated with calcite, magnesite, and hematite, respectively. Studies have shown that the distribution of heavy metals in CG has specific regional and geological characteristics [32,33]. For example, heavy metals in southern China are more enriched compared to those in northern and northwestern regions. CG is considered commercially worthless due to its inactive SiO_2 and Al_2O_3 with very weak cementitious properties; thus, it requires activation through calcination.

2.2. FA

Fly ash (FA) is a by-product of coal combustion, composed primarily of oxide and silicate minerals. The main chemical composition ranges of FA samples from ten countries or regions are shown in Fig. 3b. Australia and South Africa exhibit higher SiO2 content, while China has the highest Al_2O_3 content. For CaO, Europe, Poland, and Türkiye display a wide range, whereas Canada, the USA, and Australia show the highest Fe_2O_3 content. Non-calcareous oxides (Al_2O_3, Fe_2O_3, and SiO_2) are considered the primary substances in the hydration reaction, with CaO acting mainly as an accelerator [34]. Coal bottom ash (CBA) is collected from the bottom of coal-fired power plant and thermal power plant boilers, with properties primarily determined by the type of coal used [35]. CBA is similar to FA in composition but has a higher density and coarser particle size. CBA usually contains high amounts of Al_2O_3, Fe_2O_3, and SiO_2, and according to research [36], it can be classified as a pozzolanic material belonging to class F.

2.3. CGS

Coal gasification slag (CGS) is a significant coal-based solid waste that has garnered considerable attention from researchers in recent years. CGS is produced during the coal gasification process and is classified into two types: coarse CGS (4–9 mm) and fine CGS (<5 mm). Coarse CGS exhibits various irregular shapes, such as smooth and irregular particles, spherical, and rod-shaped, while fine CGS appears as particles, flocculent, and spherical shapes. As a primary coal chemical residue, both coarse and fine CGS contain SiO_2, CaO, Fe_2O_3, and Al_2O_3. Unlike CG and FA, CGS has a high content of Fe_2O_3 and carbon, especially in fine CGS. Consequently, due to the high residual carbon and impurity content, the comprehensive utilization ratio of CGS remains low [37–39].

3. Pretreatment of CBSW

3.1. Physical crush and edulcoration

Coal-based solid waste (CBSW) typically undergoes pretreatment before being used as a building material to enhance its purity and activity. Common pretreatment methods include crushing and impurity removal, especially for coal gangue (CG) and coal gasification slag (CGS), due to their oversized particles and high carbon content.

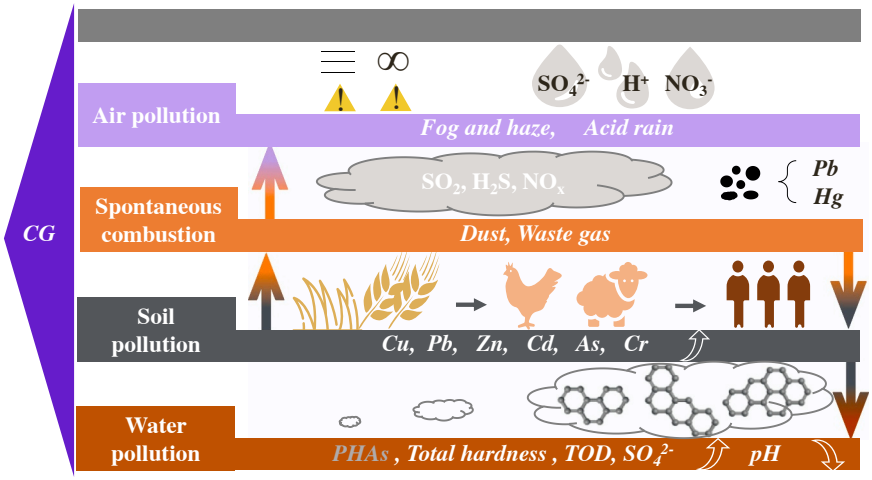

Fig. 1. The environmental risks of coal gangue.

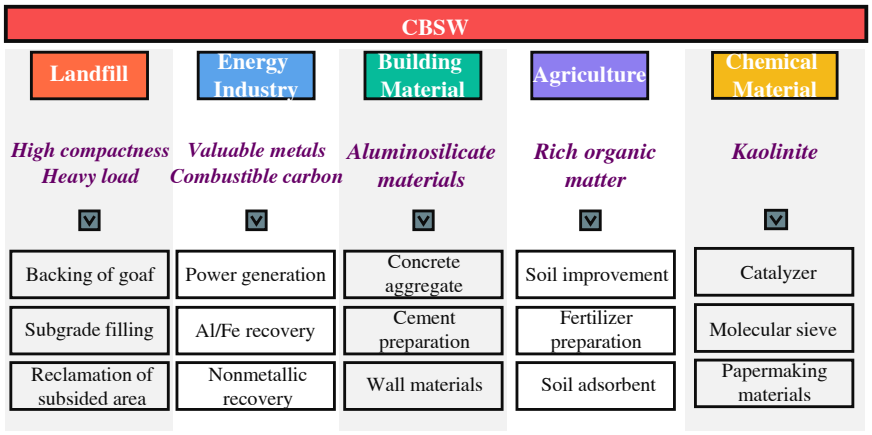

Fig. 2. The utilization of coal-based solid waste.

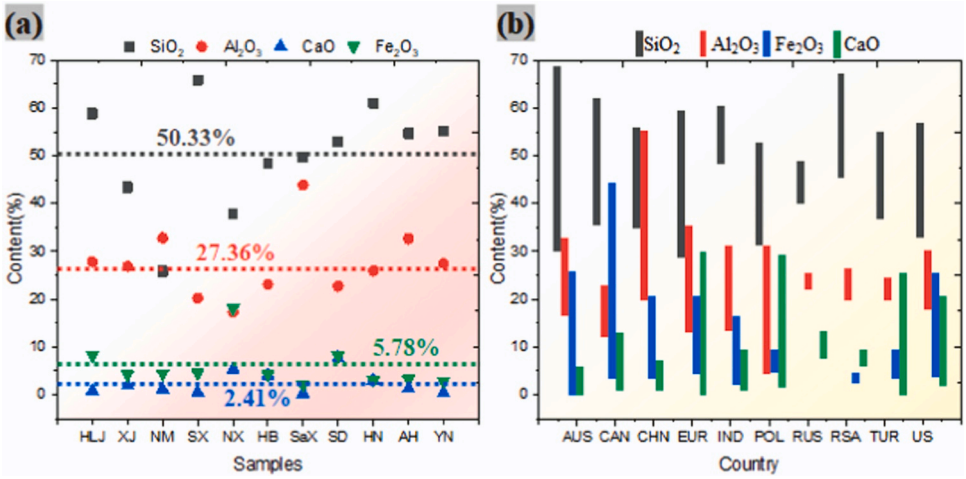

Fig. 3. The main chemical compositions of CG (a) and FA (b) [25–34].

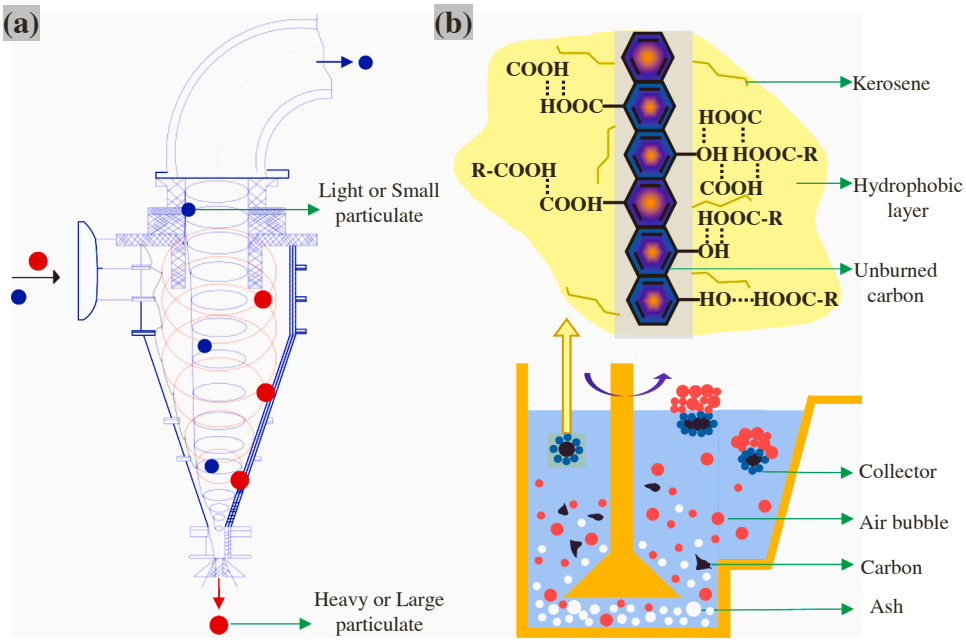

Fig. 4. The typical physical (a) and chemical (b) separation of CBSW [44–46].

CG contains inert SiO_2 and Al_2O_3 with weak cementitious properties, as its silicon-alumina phase is stable. Mechanical activation has proven effective in altering the reactivity of CG by modifying its kaolinite structure. Research indicates that mechanical grinding reduces the polymerization degrees of [SiO_4] and [AlO_6] [40]. During mechanical crushing, kaolinite, muscovite, and calcite are disrupted, while quartz retains its structure even after activation. Ball mill tests show that the structural stability of CG decreases in the order of kaolinite, calcite, and muscovite [41]. The impact and compression between CG and grinding media not only crush and separate CG particles but also increases their surface area and dehydroxylation degree [42]. The improved activity of CG through physical crushing is attributed to reduced particle size, increased surface area, and aluminum enrichment. However, some scholars argue that the kaolinite layer structure does not significantly change without calcination [43]. Therefore, a combined activation method for CBSW is necessary.

Crushing and screening processes for coal-based solid waste (CBSW) achieve the necessary particle size requirements. According to Chinese standard GB/T1596–2017 and American ASTM C618, fly ash used in cement production must have appropriate levels of free water, loss on ignition, and surface area. Coal gangue (CG) and coal gasification slag (CGS) contain varying amounts of carbon due to geological conditions and incomplete coal gasification reactions. Therefore, separating and enriching residual carbon in CBSW through physical (gravity concentration) and chemical (flotation) methods is essential. Gravity concentration separates CGS into concentrate and tailings using centrifugal force and sedimentation (Fig. 4a). The feed is injected into a cyclone under pressure, causing the concentrate (high carbon content) and tailings (high ash content) to separate based on gravity and particle size. Heavy or large particles drop from the underflow outlet, while light or small particles rise to the overflow.

For finer particles, foam flotation (Fig. 4b) is typically used to enrich residual carbon in CGS [44,45], as cyclones are ineffective for particles smaller than 0.125 mm. Collectors, stirring speed, and operation time influence the flotation separation of carbon from CGS. Kerosene, with a flotation recovery of approximately 60 %, is an effective collector that enhances particle hydrophobicity due to the adsorption of the benzene ring skeleton on CGS. Given the severe oxidation of unburned carbon on the CGS surface, a combined collector has been developed to address this issue. A mixture of kerosene and oleic acid in a 7:3 ratio improves carbon collection from CGS. This synergy between the benzene ring skeleton of kerosene and the polar groups of oleic acid enhances the hydrophobicity of carbon in CGS, increasing the carbon enrichment rate in flotation concentrate [46]. Research also shows that a mixed collector containing dodecylamine polyoxyethylene ether (AC1201) and kerosene effectively separates carbon from ash. AC1201 selectively disperses to carbon, with a higher exothermic value during the wetting process than kerosene [47].

3.2. Thermal activation

Coal gangue (CG) has the lowest pozzolanic activity and the highest content among coal-based solid wastes (CBSW). Therefore, thermal activation is employed to enhance its reactivity. This process involves the phase transformation of kaolinite ($Al_2O_3{\cdot}2SiO_2{\cdot}2\,H_2O$) at high temperatures and the combustion of organic materials, making thermal activation a promising technology for increasing the pozzolanic activity of CG. The primary equipment for thermal activation includes conventional furnaces, fluidized beds, and microwave furnaces. The activation temperature significantly influences the mineral composition of CG. The pozzolanic activity of CG gradually increases from around 450°C, sharply rises between 450°C and 570°C, and reaches its maximum value at approximately 800°C [48]. At high temperatures, kaolinite transforms into metakaolin ($Al_2O_3{\cdot}2SiO_2$), with its flake and layered structures becoming an amorphous glassy state, losing their long-range order. The dehydroxylation and disorder of metakaolin, caused by the reorganization of the Al-O network, enhance the reactivity of the transition phase metakaolin [49]. However, as the temperature increases beyond 1000°C, metakaolin transforms into mullite ($3Al_2O_3{\cdot}2SiO_2$), reducing its reactivity. The schematic diagram of kaolinite dehydrogenation is shown in Fig. 5 [50]. Major carbonate minerals, such as calcium carbonate ($CaCO_3$) and anhydrite ($CaSO_4$), decompose at 650 °C and 900 °C, respectively. When the temperature exceeds 1000 °C, CaO reacts with SiO_2 and Al_2O_3 to form feldspar ($CaAl_2Si_2O_8$), anorthite ($Ca_2Al_2Si_2O_7$), and calcium silicate ($CaSi_2O_3$).(Fig. 6)

Microwave activation demonstrates potential for enhancing activation performance due to its rapid and uniform internal heating [51]. Research indicates that microwave activation accelerates the phase transformation process by more than ten times compared to conventional heating methods [52]. Structural and micro-compositional analyses reveal that mortar containing microwave-activated coal gangue significantly improves the strength of cement-microwave activated-coal gangue mixtures. Microwave activation decomposes inactive kaolinite into active substances, rendering the mineral particles of CG rounder and more compatible with the mortar matrix. In the mortar, calcium silicate hydrate (C-S-H), the main hydration product, gradually increases with age. The depolymerization of metakaolin in an alkaline solution promotes the secondary hydration reaction of active Al_2O_3 and SiO_2, substantially enhancing the mechanical strength of the mortar [53].

3.3. Chemical activation

Various investigations into the mechanism of chemical activation of coal bottom ash (CBSW) and its reaction properties have been conducted, typically following either thermal activation or physical crushing to reduce cement consumption [54]. Chemical activation involves enhancing the reactivity of CBSW, which facilitates the disruption of Si-O-Si and Al-O-Al covalent bonds and promotes the formation of three-dimensional polymerized aluminates. Different types, dosages, and ratios of activators are introduced to activate coal gangue (CG), fly ash (FA), and copper converter slag (CCS). The chemical activation process for CBSW can be categorized into three stages: dissolution, depolymerization, and condensation [50,55]. Fig. 7 illustrates a descriptive model of alkali activation for FA [56]. As depicted in Fig. 7a, FA typically consists of vitreous spherical particles of varying sizes, often hollow, some containing smaller particles within. Initially, the activator attacks a point on the FA surface, dissolving the Si-Al-O structure, which expands the surface and causes erosion inside and out (Fig. 7b).

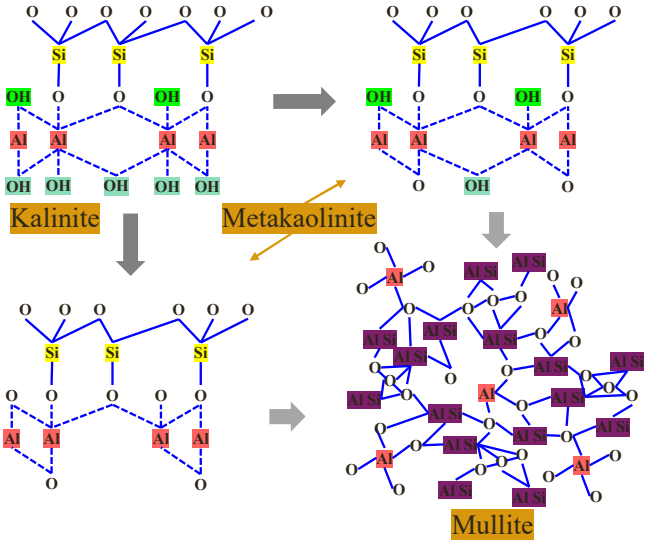

Fig. 5. Schematic diagram of dehydrogenation of kalinite [50].

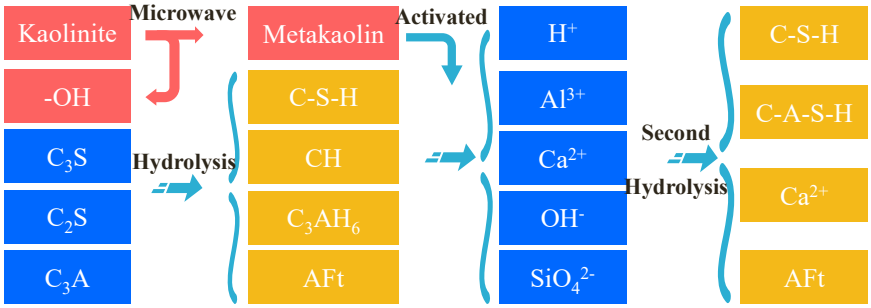

Fig. 6. Schematic of the hydration process of activated coal gangue powder [53].

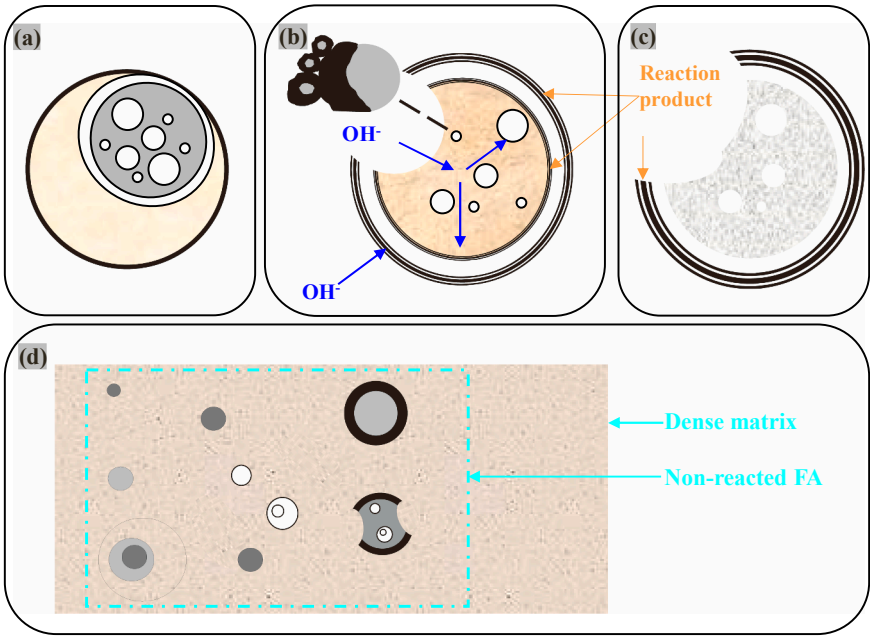

Fig. 7. Descriptive model of the alkali activation of FA [56] (a) initial chemical attack of a particle, (b) bi-directional alkaline attack, (c) cementitious matrix and (d) the highly compacted paste.

However, the strength of the sample does not significantly increase during this dissolution phase. In the subsequent stage, there is a substantial precipitation of a metastable gel [57]. Over time, the aluminum-rich phase shifts gradually to the silicon-rich phase, increasing the Si/Al ratio as the new gel slowly dissolves in the alkaline environment and incorporates silicon into the structural framework [58, 59], a phase sometimes termed silicon incorporation. The presence of soluble silica and activator contributes significantly to forming sodium aluminosilicate gel, creating a cementitious matrix (Fig. 7c). Ultimately, during the chemical activation of FA, the matrix transforms into a highly compacted paste with a high Si/Al ratio (Fig. 7d).

Since the discovery of sodium hydroxide as a catalyst for cement hydration [60], extensive research has been conducted on the types and dosages of alkali activators. Generally, the reaction mechanism of alkali-activated binders is categorized into two types: activation of calcium-rich raw materials and activation of calcium-free or low-calcium raw materials. The former predominantly yields aluminum-calcium silicate hydrate and calcium silicate hydrates (N(C)ASH and CSH), while the latter primarily forms amorphous zeolite phase polymers [59]. The reaction product from calcium-rich raw materials is aluminum-calcium silicate hydrate (CASH) gel, whereas silica-rich materials produce sodium (calcium) aluminum–silicate hydrate (N(C)ASH gel) [61]. Table 1 outlines the effects of common activators on CBSW.

4. Performance of concrete with CBSW

4.1. Performance of concrete with CG

Coal gangue (CG) is commonly utilized as an aggregate in concrete, with considerations focusing on workability, strength, shrinkage, and durability. Incorporating spontaneously combusted or unburned coal gangue has been found to decrease the slump of concrete due to its loose, porous, and flaky particle structure compared to natural aggregates, resulting in variable performance [71]. Regarding strength, concrete structures containing CG generally exhibit lower strength compared to those made with natural aggregates [72]. Analysis of the interfacial transition zones (ITZs) reveals that the porous surface characteristics of CG increase aggregate water absorption and reduce the water-binder ratio at ITZs, thereby lowering hydration levels and making ITZs the weakest areas in CG concrete [73]. Concrete shrinkage primarily stems from the shrinkage of the cement paste [74]. Adding CG typically increases concrete shrinkage due to higher water absorption and reduced stiffness. According to Mao et al. [75], coarse aggregates significantly increase concrete shrinkage strain, with fine aggregates having a lesser impact; for instance, using 100 % coarse aggregates resulted in a strain increase of 64.9 %–72.6 %, whereas for 100 % fine aggregates, it was 37.4 %–43.1 %. Moreover, fine aggregates accelerate the rate of shrinkage development in concrete.

Table 1
The effects of common activators on CBSW.

CBSW type	Pretreatment of CBSW	Activator properties	Reaction properties	Reference
CG	Calcined CG at 700 °C for 2 h	Sodium hydroxide and sodium silicate, and the optimal ratio of the above activator is 1:1.5–1:2	The modulus of sodium hydroxide is proportional to the compressive of CG, and the production of zeolite facies crystallization contributes to its compressive strength.	[62]
	Calcined CG at 750 °C for 4 h	Soluble glass with modulus of 3.4	The weight fraction of calcined CG ≤30 %, cementitious material has little strength loss. The weight fraction of calcined CG= 40–50 %, its strength is still higher than 30 MPa. The weight fraction of calcined CG > 60 %, its strength has a significant decrease.	[63]
	Calcined CG	Na_2SiO_3 and NaOH	Na_2SiO_3 can be hydrolyzed to NaOH and soluble silica gel, and provide active SiO_2 to react with Ca^{2+} and Al^{3+} to produce CSH	[64]
FA	F type FA	Calcium carbide slag (19 %) and sodium silicate (1, 3 and 5 %)	Co-activated FA geopolymer by calcium carbide slag and sodium silicate have higher compressive strength than that of a single activator, and the co-activation system significantly promotes CSH content.	[65]
	F type FA	Na_2SiO_3/ NaOH (KOH/ Ca (OH) $_2$)	Alkali activator types and curing conditions have a low influence on the compressive strength of geopolymer as the alkali activator and FA ratio reaches 0.4. NaOH-based geopolymer exhibits higher compressive strength than that of KOH-based geopolymer and Ca $(OH)_2$-based geopolymer	[66]
	type V siliceous FA	Sodium carbonate, potassium sodium silicate, potassium citrate and sodium oxalate	All activators accelerate early setting and compressive strength except the potassium citrate. Using activators promotes the pH values and reduces the calcium concentrations, resulting in a faster reaction of alite.	[67]
CCS	Coal gasification fly ash	NaOH with industrial Na_2SiO_3 solution	The geopolymer was activated at 8 mol/L NaOH, Na_2SiO_3, and a liquid/solid ratio of 0.33.	[68]
	Coarse and fine gasification slags	Hydrated lime	The usage of lime activates the SiO_2 and Al_2O_3 of CCS to generate cementitious products, and thus promotes its strength.	[69]
	Integrated gasification combined cycle slag and fine coal gasification slag	Na_2SiO_3	The geopolymer reaches 80 MPa.	[70]

Various methods have been explored to enhance CG aggregate properties and mitigate its adverse effects on concrete performance. Cement slurry coating has been shown to enhance compressive strength, splitting tensile strength, and flexural toughness of concrete (Fig. 8a). Research on mechanically treated CG aggregate reveals improvements when coated with cement, epoxy resin, fly ash, silica fume, and calcined CG [71]. Concrete incorporating 100 % modified CG aggregate exhibits significantly improved compressive strength (13.0 %–32.9 % increase) and splitting tensile strength (7.4 %–39.6 % increase), with cement-modified CG showing the most substantial enhancements.

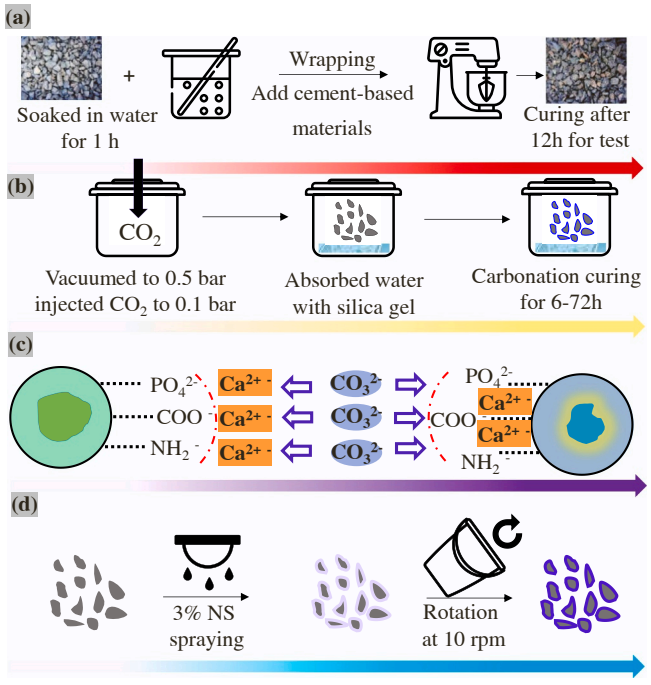

Fig. 8. Typical aggregate reinforcement techniques [71,76–78] (a) cement slurry coating, (b) CO_2 curing, (c) microbially-induced carbonate precipitation and (d) nano-silica spraying.

Cement-modified CG aggregates improve ITZ hardness by forming a protective shell, thereby enhancing concrete mechanical properties.

Methods such as CO_2 curing (Fig. 8b), microbially-induced carbonate precipitation (Fig. 8c), and nano-silica spraying (Fig. 8d) are employed to reinforce concrete performance [76–78]. CO_2 and microbial treatments result in calcium carbonate mineral deposits on aggregate surfaces, reducing porosity and enhancing surface strength. Nano-silica spraying improves mechanical and durability properties by significantly enhancing new ITZs. Comparison studies show that nano-silica treatment outperforms carbonation in enhancing concrete mechanical properties [76]. While the performance of individually reinforced aggregates still lags behind natural aggregates, composite treatment approaches bring CG aggregate performance closer to that of natural counterparts.

Coal gangue (CG) serves not only as aggregates but also as an active admixture to substitute cement. Its main source of activity stems from thermal decomposition, which significantly influences early-age cement reactivity. Guan et al. [79] demonstrated that microwave-promoted CG exhibited a 72.5 % increase in compressive strength and a 42.32 % increase in flexural strength of mortar at temperatures ranging from 600 ℃ to 700 ℃. Secondary hydration of calcium silicates (C-S-H gels) and formation of Aft crystals filled macropores and capillaries, while non-hydrated CG particles acted as micro-aggregates, enhancing strength development. Furthermore, research [80] indicated that extending the thermal decomposition holding time notably boosted CG activity, especially at varied temperatures. Although CG powder's thermal decomposition reduces cement mortar fluidity, optimal temperature and holding time can mitigate this effect. Investigating cooling conditions, room temperature cooling was found to yield the most reactive CG compared to rapid, slow, and water-cooling modes. CG powder also reduces harmful pores (>100 nm) while increasing benign pores (<100 nm) in hardened cement paste [81]. Optimizing CG thermal activation offers potential as both aggregate and cement substitute, promising cost reduction. However, achieving a balance between enhancing CG performance and realizing environmental, ecological, and low-carbon benefits remains a crucial focus.

4.2. Performance of concrete with FA

Fly ash (FA) is commonly used as a mineral admixture, significantly influencing various properties of concrete such as fresh characteristics, strength, and durability. Changes in fluidity and setting time are notable with varying FA content. This can be attributed to several factors: FA's lower density compared to cement increases paste volume; FA dilutes cement particles, reducing flocculation; and FA's lower reactivity slows early-age hydration product formation [82]. Fig. 9a illustrates the fresh properties of FA concrete, highlighting improved fluidity due to the ball-bearing effect of its spherical particles compared to concrete without FA [83,84]. However, excess FA above optimal conditions can reduce fluidity as fine particles require more water for wetting [85]. Fig. 9a also depicts conflicting trends in concrete slump: generally, FA enhances slump due to its properties [86], but incomplete carbon combustion can produce irregular, coarse particles that decrease slump [87]. Fig. 9b demonstrates the 28-day compressive strength of FA concrete, showing varying trends across studies. In most cases, FA enhances concrete strength by filling pores and improving structural compactness through its filling and morphological effects. Additionally, FA's SiO_2, Al_2O_3, and other components react with $Ca(OH)_2$ to form C–S–H gel, promoting concrete hydration [88]. However, some studies, like that by Wang et al. [89], suggest FA may reduce compressive strength due to its limited pozzolanic activity.

Chloride-induced corrosion is a significant issue affecting concrete structures and is one of the most extensively studied environmental deterioration phenomena. The resistance of concrete structures to chloride ion penetration is primarily related to their porosity and water absorption properties [90]. It is widely recognized that fly ash (FA) enhances the permeability resistance to chloride ions. The calcium-silicate-hydrate (C-S-H) phase formed from FA has a lower calcium-silicon ratio compared to that of ordinary Portland cement (OPC) [91], and the addition of FA increases the volume of Friedel's salt and the chloride binding capacity of cement [92]. The inclusion of FA reduces the content of alkali ions (Na^+ and K^+) and hydroxyl ions in the pore solution [93], which is beneficial since the alkali ions in the pore solution of concrete promote the hydroxyl ion (OH^-) content. OH^- can replace Cl^- ions bound to C-S-H and Friedel's salt. Fig. 10 illustrates the chloride binding isotherms of OPC with FA paste exposed to NaCl, $CaCl_2$, and $MgCl_2$ [94]. As shown, in NaCl solution, when the cement replacement ratio with FA reaches 15 % and 30 %, the amount of bound chlorides increases by 176 % and 216 %, respectively, compared to OPC. Similar trends are observed in $CaCl_2$ and $MgCl_2$ solutions. This increase is primarily due to the pozzolanic reactions of FA, particularly its high Al2O3 content, which contribute to the formation of monosulfoaluminate (AFm) phases and C-S-H [95]. AFm aids in the formation of chloride-bearing compounds, such as Friedel's salt, which is the primary form of chemical chloride binding. Concurrently, C-S-H enhances durability due to its capacity for physical chloride binding.

FA not only augments the resistance of concrete to chloride ion erosion but also improves its resistance to sulfate attack, water absorption and freeze-thaw performance. This improvement is primarily attributed to FA's ability to optimize the pore structure of concrete and

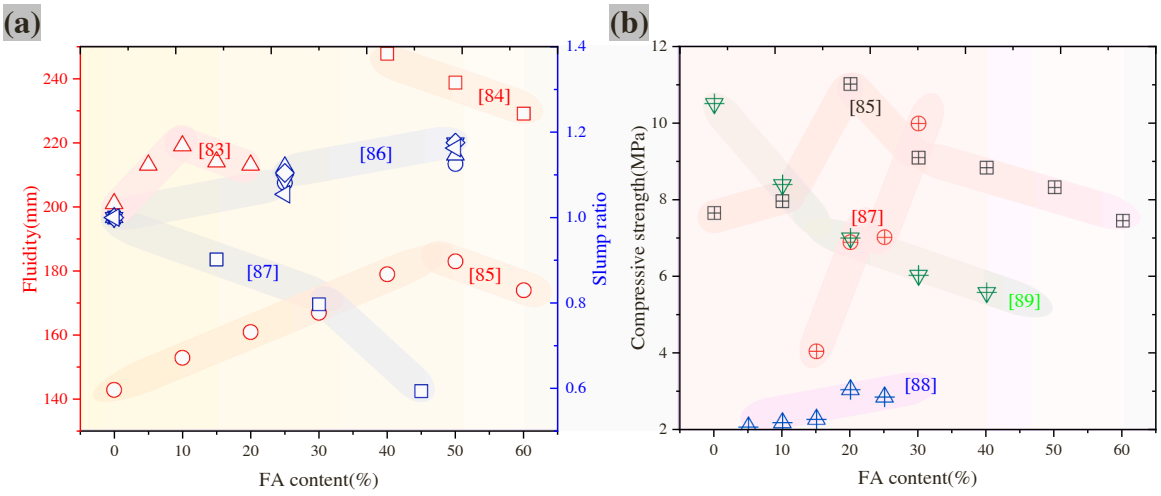

Fig. 9. The fresh properties (a) and compressive strength (b) of concrete with FA [83–89].

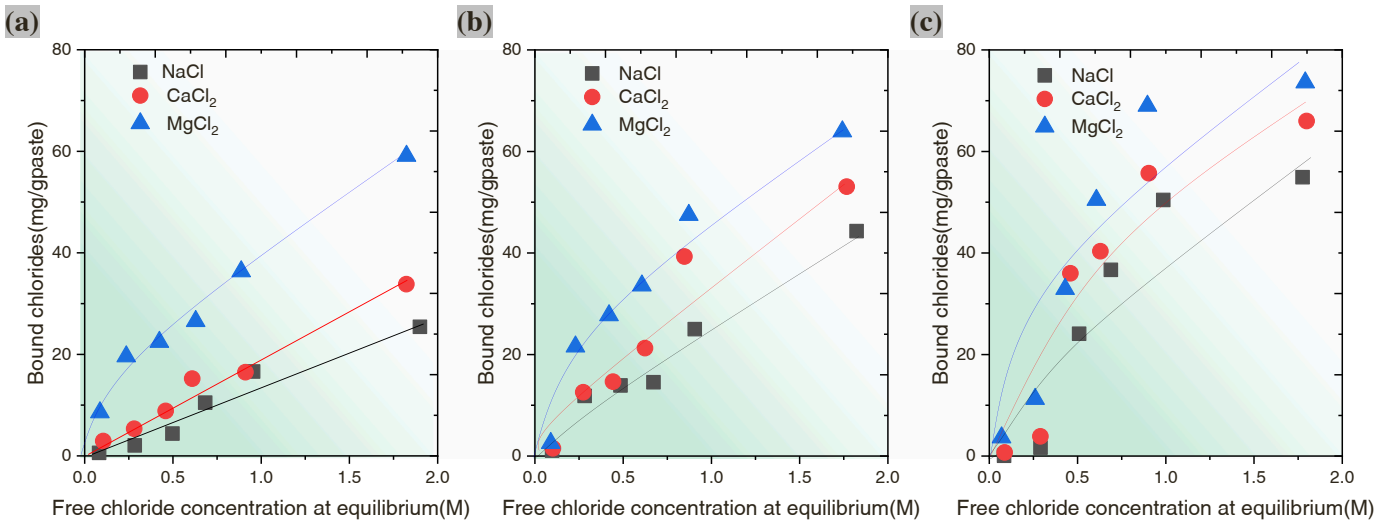

Fig. 10. The chloride binding isotherms of ordinary Portland cement with FA paste exposed to NaCl, $CaCl_2$ and $MgCl_2$(a) ordinary Portland cement, (b) 15 % FA, (c) 30 % FA [94].

enhance the compactness of the matrix [96]. As illustrated in Fig. 11, the impact of FA on the freeze-thaw cycle and pore structure of concrete is elucidated. The infiltration of water into concrete leads to freezing expansion, resulting in the formation of micro-cracks and structural damage [97,98]. In Fig. 11a and b, with an increasing number of freeze-thaw cycles, there is a corresponding escalation in the loss of

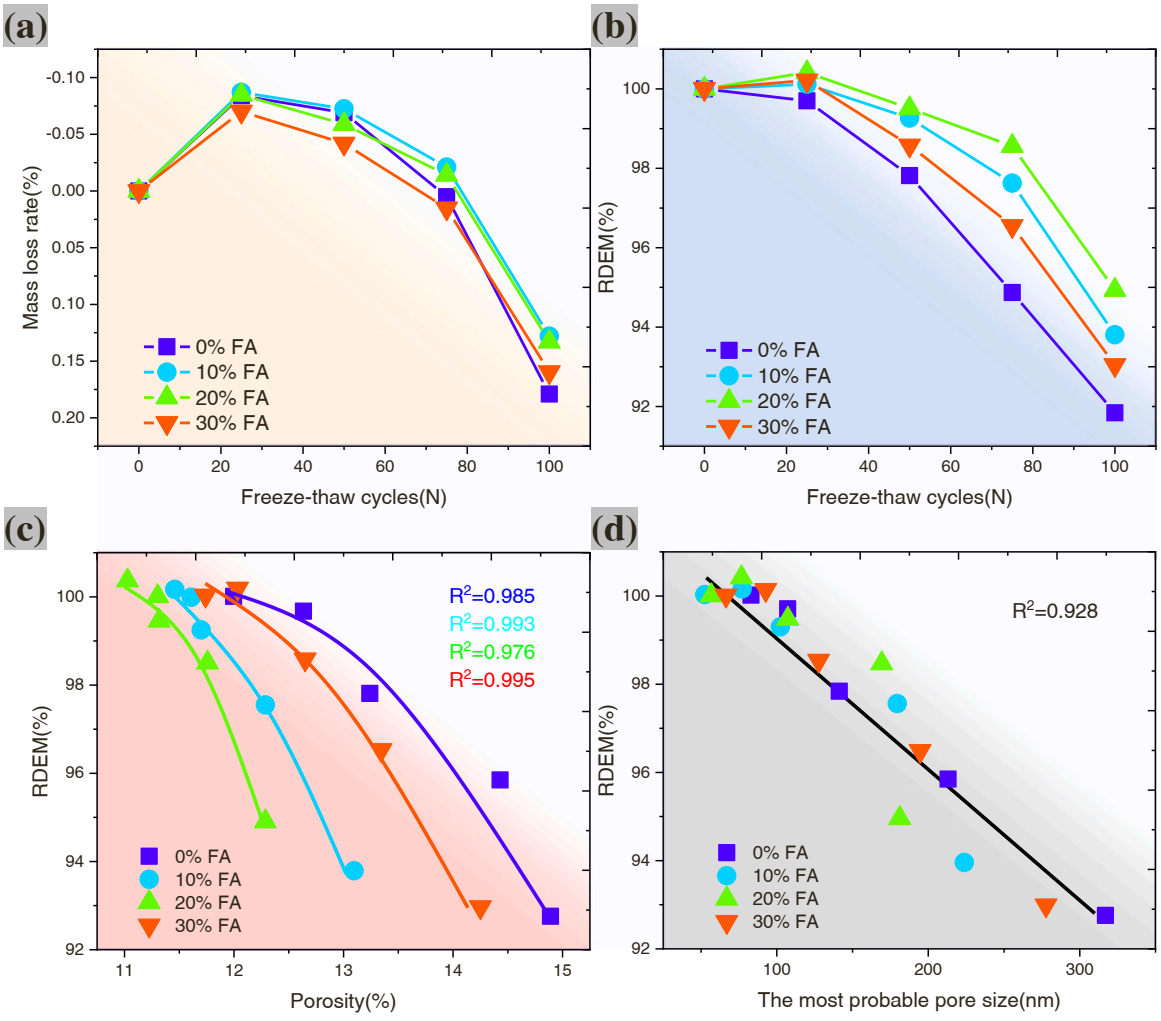

Fig. 11. The influence of FA on freeze-thaw cycle and pore structure of concrete (a) mass loss ratio, (b) RDEM of concrete, (c) RDEM of concrete with the porosity, (d) RDEM of concrete with the most probable pore size [99].

concrete weight and relative dynamic modulus of elasticity (RDEM). The incorporation of FA demonstrates efficacy in augmenting the freeze-thaw resistance of concrete. With an increasing dosage of FA, the freeze-thaw resistance first strengthens and then decreases. Concrete with a 20 % FA exhibits an optimal frost resistance, which is consistent with the analysis in Fig. 11c, where the porosity is lowest. The nuclear magnetic resonance analysis indicates a negative correlation between the RDEM and the most probable pore size, and the inclusion of FA significantly mitigates the size of the most probable pore diameter [99].

4.3. Performance of concrete with CGS

Currently, the application of coal gasification slag (CGS) is limited, primarily due to its high carbon content and notable particle size disparity, despite the potential pozzolanic activity of the active Al_2O_3 and SiO_2 present within CGS. As shown in Table 2, the optimal addition percentage of CGS in concrete typically does not exceed 30 %. Research consensus indicates that CGS can enhance the flowability of concrete. Compared to coal gangue (CG) and fly ash (FA), CGS exhibits higher porosity and carbon content, leading to increased water absorption and a consequent decrease in mechanical properties. However, the impact on durability varies and may be attributed to the basic properties of CGS, such as fineness, carbon content, and active components. The use of activators (e.g., $CaCl_2$ and Na_2SO_4) can enhance the reactivity of CGS, facilitating its application in filling materials. Overall, research on CGS remains relatively limited, and addressing the impact of carbon content on building materials will be a focal point for future investigations.

Table 2
The performance of CGS on building materials.

Properties	Main components	Effect of CGS on cementitious material	Ref.
Fine CGS	53.77 % SiO_2, 17.04 % Al_2O_3 and 10.45 % Fe_2O_3	As CGS doping increases from 0 % to 10 %, pastes fluidity increases from 250 mm to 263 mm and yield stress decreases from 2.235 Pa to 0.789 Pa.	[100]
CGS has a specific surface area of 445 m^2/kg and a density of 2550 kg/m^2	47.78 % SiO_2, 13.63 % Al_2O_3, and 16.15 % CaO	As CGS doping increases from 0 % to 30 %, pastes fluidity increases from 155 mm to 175 mm, yield stress decreases approximately from 49 Pa to 35 Pa and plastic viscosity decreases approximately from 0.87 Pa to 0.73 Pa.	[101]
CGS exhibits a specific surface area of 487 m^2/kg and an apparent density of 3020 kg/m^3.	29.25 % SiO_2, 18.12 % Al_2O_3 and 21.41 % CaO	When the shear rate was 100 s^{-1}, the low CGS fineness (median particle size was 5.2 μm) reduced viscosity approximately from 4.3 Pa·s to 2.7 Pa·s of the pastes.	[102]
Coarse slag is used after grinding treatment	47.78 % SiO_2, 13.63 % Al_2O_3 and 16.15 % CaO	The introduction of 10 % CGS enhanced the microstructure and subsequent compressive strength (the strength of 1 d, 7 d and 28 d increased by 7.1 %, 6.9 % and 5.4 %, respectively).	[103]
CGS is subjected to flotation technology for carbon removal	49.35 % SiO_2, 19.01 % Al_2O_3, 10.06 % Fe_2O_3 and 11.38 % CaO	CGS ground at 20 min presented the finest particle size, and the corresponding geopolymer had the highest compressive strength (19.42 MPa).	[104]
The raw CGS has a coarse particle size	30.90 % SiO_2, 11.01 % Al_2O_3, 23.20 % Fe_2O_3 and 17.19 % CaO	Including 1 % $CaCl_2$ enhances the unconfined compressive strength (UCS) of CGS-based cementitious backfill materials.	[105]
CGS with a particle size distribution of 0.074 mm ~2.36 mm	30.94 % SiO_2, 11.01 % Al_2O_3, 23.22 % Fe_2O_3 and 17.19 % CaO	The early strength development of CGS activated by sodium sulfate is rapid, but in the later stages, the formation of AFt leads to a decline in strength.	[106]

5. Carbon reduction of concrete with CBSW

The construction industry ranks second only to industrial activities in global CO_2 emissions, prompting significant scholarly interest in enhancing energy efficiency and reducing carbon output within this sector. As previously noted, the utilization of coal-based solid waste (CBSW) emerges as a promising strategy to decrease reliance on natural resources, thereby promoting sustainability in construction practices. Moreover, integrating CBSW can enhance specific material properties, such as thermal insulation and durability, potentially extending the operational longevity of concrete structures while concurrently mitigating carbon emissions [107–111]. Additionally, the adoption of CBSW contributes to a reduction in cement consumption, which is critical since producing each ton of cement generates an average of 0.79 tons of CO_2 [112].

Concrete is the world's most important and widely used construction material, and the CO_2 emissions generated during the material selection and preparation of concrete structures constitute a significant proportion of global emissions. As mentioned, utilizing CBSW materials for building purposes offers substantial low-carbon benefits. Therefore, understanding low-carbon technologies in the preparation process of CBSW is particularly important. Key carbon reduction technologies in this process include carbon dioxide injection, carbon dioxide curing, 3D printing, and prefabrication technologies [113–116]. This paper primarily focuses on the increasingly popular research area of carbonation curing technology in preparing concrete with CBSW, aiming to enhance understanding of carbon reduction in coal-based solid waste.

The mechanism of carbonation in cementitious materials is illustrated in Fig. 12. The carbonation process encompasses three stages: gas phase, pore fluid, and solid phases. In the gas phase, CO_2 gas diffuses, permeates, and dissolves. CO_2 entering the pore fluid phase undergoes ionization, forming HCO_3^- and CO_3^{2-}. These ions react with Ca^{2+} and SO_4^{2-} produced by the dissolution of C_2S and C_3S, leading to the formation of calcium silicate hydrate (C-S-H) and calcium carbonate ($CaCO_3$). The formation of $CaCO_3$ may involve unstable forms such as vaterite and aragonite. Additionally, C-S-H undergoes secondary carbonation, yielding $CaCO_3$ and silica hydrate (SH) gel [117–119].

The impact of carbonation curing on concrete building materials is influenced by factors such as the type of raw materials, CO_2

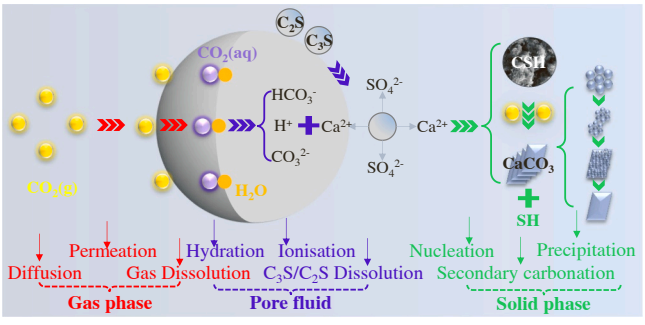

Fig. 12. The mechanism for accelerated carbonation [117].

concentration and pressure, and pre-curing effects. This section focuses on the macroscopic performance and microscopic structure of CBSW concrete subjected to carbonation curing.

5.1. The influencing factors of carbonization curing

CO_2 concentration, carbonization pressure, carbonization time, and carbonization temperature can affect the rate and extent of CO_2 absorption, thereby influencing the carbonation reaction process and the development of the mixed slurry's strength [120]. Low CO_2 concentrations (0.04 %) may result in incomplete carbonation reactions, whereas high concentrations (20 %) promote $CaCO_3$ precipitation, which can block pores and diffuse within the cementitious matrix, thus enhancing the carbonation reaction. Early-formed $CaCO_3$ also provides nucleation sites for subsequent carbonation reactions. Cui et al. [121] found that concrete carbonation depth increased with rising CO_2 concentration, with the most significant increase occurring when the concentration rose from 2 % to 10 %. However, when the concentration exceeded 20 %, the rate of increase in carbonation depth significantly decreased (Fig. 13a). Shi et al. [122] investigated different CO_2 concentrations (0.04 %, 3 %, and 20 %) and found that carbonation depth increased from 0 mm to 4.18 mm as the concentration increased.

Increasing CO_2 pressure enhances CO_2 solubility, accelerates the carbonation reaction rate, and increases compressive strength and growth rate [123] (Fig. 13b). The diffusion rate of Ca^{2+} is a key factor in determining the overall carbonation rate [124]. However, Ca^{2+} diffusion is less affected by pressure, resulting in a lower final carbonation rate [125]. Extending carbonization time ensures a sufficient reaction, significantly increasing carbonation depth and CO_2 absorption per unit mass of cement [126] (Fig. 13c). Sufficient carbonation allows $CaCO_3$ crystals to attach to or embed within the C-S-H gel, forming strong bonds that enhance early cement mortar strength (from 0.7 MPa to 12.6 MPa in 2 days) [127]. Carbonation curing also improves the bond between aggregate and mortar by filling voids and microcracks in the interfacial transition zones (ITZs), thereby reducing ITZ defects [128].

Temperature significantly influences the carbonation process. According to Ukwattage et al. [129], CO_2 absorption increases with rising temperatures (20 °C to 80 °C), peaking at 60 °C before decreasing. Beuer [130] studied the effects of carbonation concentration, pressure, and temperature on CO_2 absorption, finding that at fixed CO_2 concentration and pressure, absorption increased with temperature (20 °C to 100 °C). Additionally, the conversion rate of calcium rose with temperature (25 °C to 175 °C), from 45 % to 65 %, likely due to faster Ca^{2+} leaching from the matrix [131] (Fig. 13d). It is worth noting that 60 °C may be the optimal temperature for FA carbonation, as higher temperatures can reduce the carbonation reaction rate [132].

In addition to the factors mentioned above, the influence of moisture content on the carbonation process should not be overlooked. There may be an optimal moisture content (water-to-solid ratio) during carbonation. Excessive moisture can readily occlude pores, thereby restricting the diffusion of CO_2 gas to the liquid film surrounding solid particles, hindering CO_2 dissolution, and Ca^{2+} leaching [145]. Conversely, insufficient moisture lacks the moist environment required for wet carbonation, significantly reducing the carbonation rate [129]. Therefore, pre-treatment emerges as a pivotal step in expediting the carbonation process. Researchers have found that pre-treatments such as ultraviolet (UV) pre-irradiation and pre-carbonization treatment can effectively reduce the moisture content of cement slurry, promote natural carbonation of cement slurry, and accelerate early hydration rates. The reduction in moisture content following UV pre-irradiation creates more pathways for CO_2 ingress into the mixed slurry, thereby enhancing CO_2 absorption [122] (Fig. 14a). Pre-carbonization treatment involves

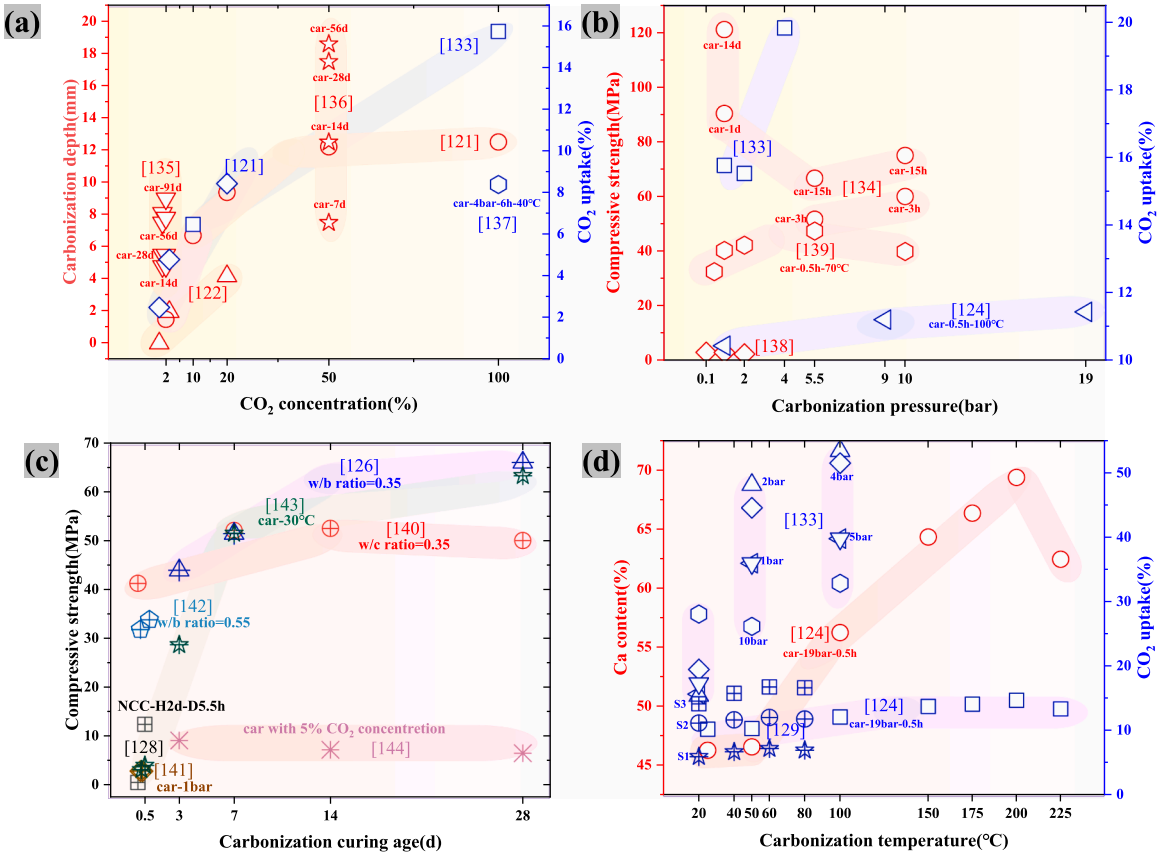

Fig. 13. The factors affecting carbonization curing (a) CO_2 concentration, (b) curing age, (c) the pressure, (d) the temperature (car: carbonization curing, NCC: normal carbonized concrete, H: hydrate, D: dry, S1、S2 and S3: fly ash sample) [121–144].

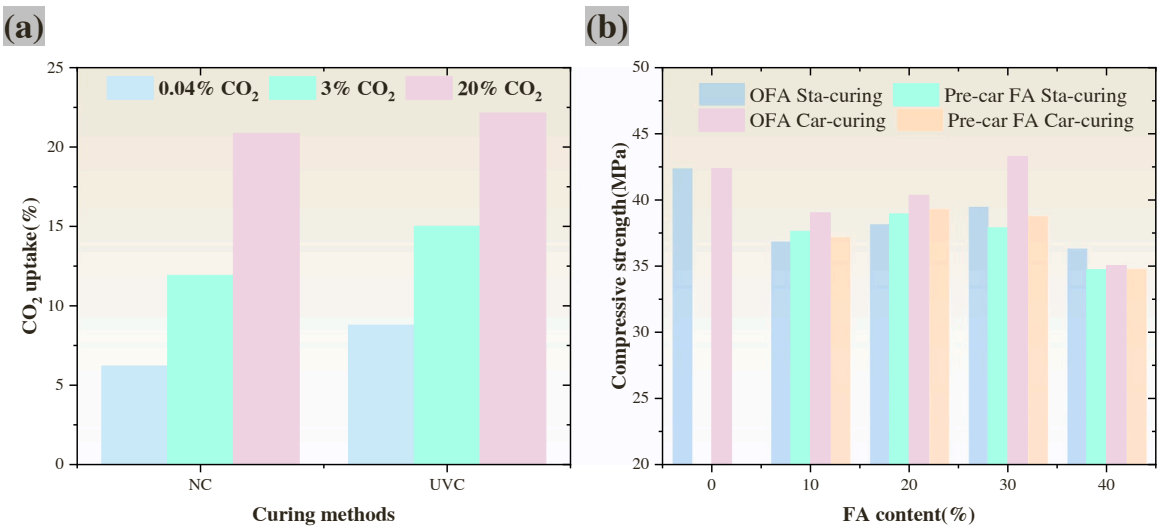

Fig. 14. The influence of pretreatment methods on compressive strength and CO_2 absorption rate [122,147] (OFA: Ordinary FA; Sta-curing: standard curing, Car-curing: carbonization curing, Pre-car: pre-carbonization).

the consumption of free CaO in FA, resulting in the formation of nano-scale carbonates on the surface, consequently accelerating the rate of the carbonation reaction [146,147] (Fig. 14b).

5.2. Performance of concrete with CBSW cured by carbonation

The influence of carbonation curing on the performance of CBSW concrete is primarily reflected in its mechanical and durability properties. While the use of CBSW may initially decrease concrete strength, carbonation curing can offset the strength loss associated with CBSW replacing cement. For instance, in FA and Portland cement systems, most FA acts as a filler, resulting in a relatively weak pozzolanic effect. Additionally, carbonation products like $CaCO_3$ can coat unreacted clinker surfaces, hindering hydration and inhibiting the development of compressive strength [148–150] (Fig. 15). Carbonation curing reduces the Ca/Si ratio of C-S-H gel, promotes the coverage of C-S-H on $CaCO_3$ surfaces, and forms a denser microstructure [151]. In FA and magnesium oxychloride cement systems, carbonation curing enhances the filling effect of $MgCO_3$ and $CaCO_3$ in pores, thereby improving the compressive strength of concrete [152]. The addition of FA reduces

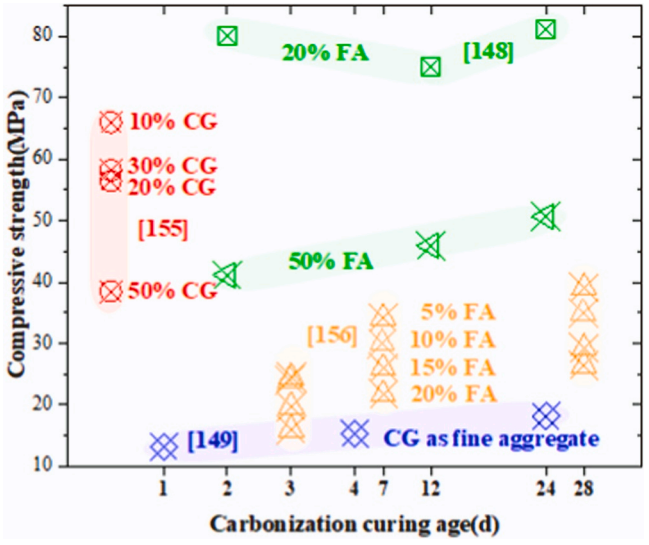

Fig. 15. Compensation for strength loss of CSBW by carbonization curing [148, 149,155,156].

unhydrated MgO content in the slurry, and the reaction between amorphous SiO_2 and $Mg(OH)_2$ forms M-S-H gel, creating a dense microstructure intertwined with needle-like phases, thereby enhancing flexural strength [153,154].

The coupling effect between CBSW and carbonation improves the durability performance of concrete. For instance, FA and CG enhance lightweight aggregate performance and reduce water absorption [157]. Prolonged carbonation curing significantly reduces concrete's water absorption and enhances impermeability [158]. Adding 10–30 % FA typically improves the frost resistance of concrete. The $CaCO_3$ formed by carbonation curing fills pores and forms a dense carbonation layer on the surface, mitigating volume expansion and freeze-thaw stress hazards caused by freeze-thaw cycles [159,160]. Carbonation curing and FA incorporation contribute to pore refinement and the formation of a carbonate protective layer, reducing Cl- migration coefficients and adsorption. The mixed formation of crystalline calcium carbonate and C-S-H results in a structure with lower permeability [161,162]. Due to the decrease in Friedel's salt content caused by the consumption of $Ca(OH)_2$ and the presence of carbonates, as well as the reduction of C-S-H gel, the chloride binding capacity of carbonation-cured FA cement slurry is significantly reduced [163] (Fig. 16a). Water evaporation caused by carbonation curing increases early drying shrinkage, while the porous structure and strong water absorption of CG help reduce the free water content in the cement slurry [164,165]. The absorbed water provides internal curing during drying, reducing water evaporation and decreasing drying shrinkage [166]. After six months of sulfate erosion, the formation of gypsum and ettringite causes expansion, with significant cracking (50 %) observed on the surface of CG-cement slurry samples [167]. Post-carbonation curing, CG-cement slurry exhibits good resistance to sulfate erosion, attributed to microstructure densification and improved impermeability [25] (Fig. 16b).

The enhancement of CBSW concrete properties through carbonation curing fundamentally results from microstructural improvements. Carbonation curing optimizes the pore structure by incorporating FA, which reduces the volume of large and medium capillary pores (10–1000 nm) [163,168]. Conversely, incorporating CG increases the number of coarse pores larger than 100 nm, significantly increasing porosity and reducing resistance to Cl^- penetration [25] (Fig. 16b). The formation of $CaCO_3$ during carbonation refines the pore size, preferentially filling gel pores and medium capillary pores, thus increasing the average pore size [169]. Regarding hydration product formation, carbonation transforms more $Ca(OH)_2$ into $CaCO_3$, which has a higher hardness and elastic modulus than $Ca(OH)_2$ and C-S-H [170,171].

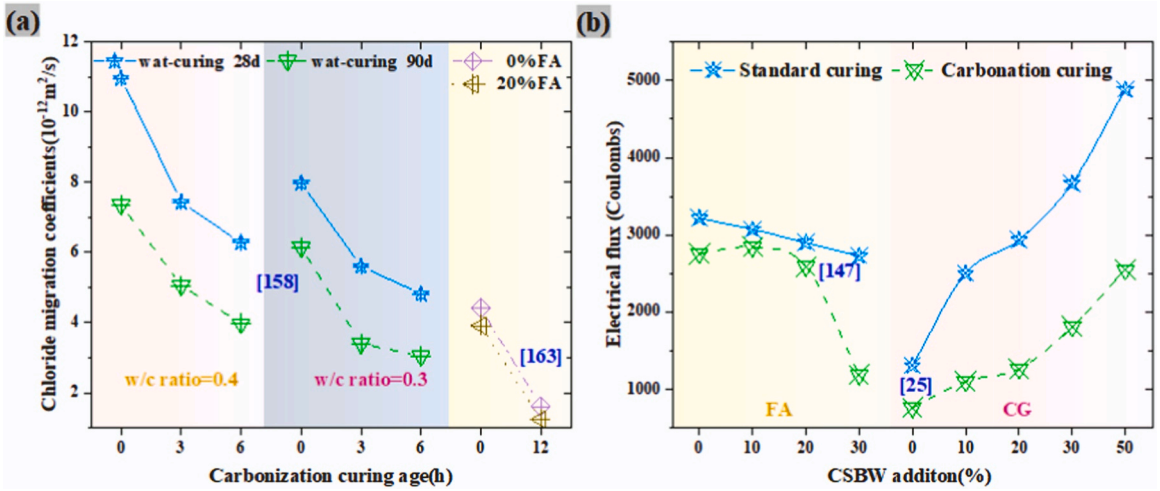

Fig. 16. The effect of carbonization curing on the chloride ion penetration resistance of CSBW [25,147,158,163] (wat-curing: curing in lime water).

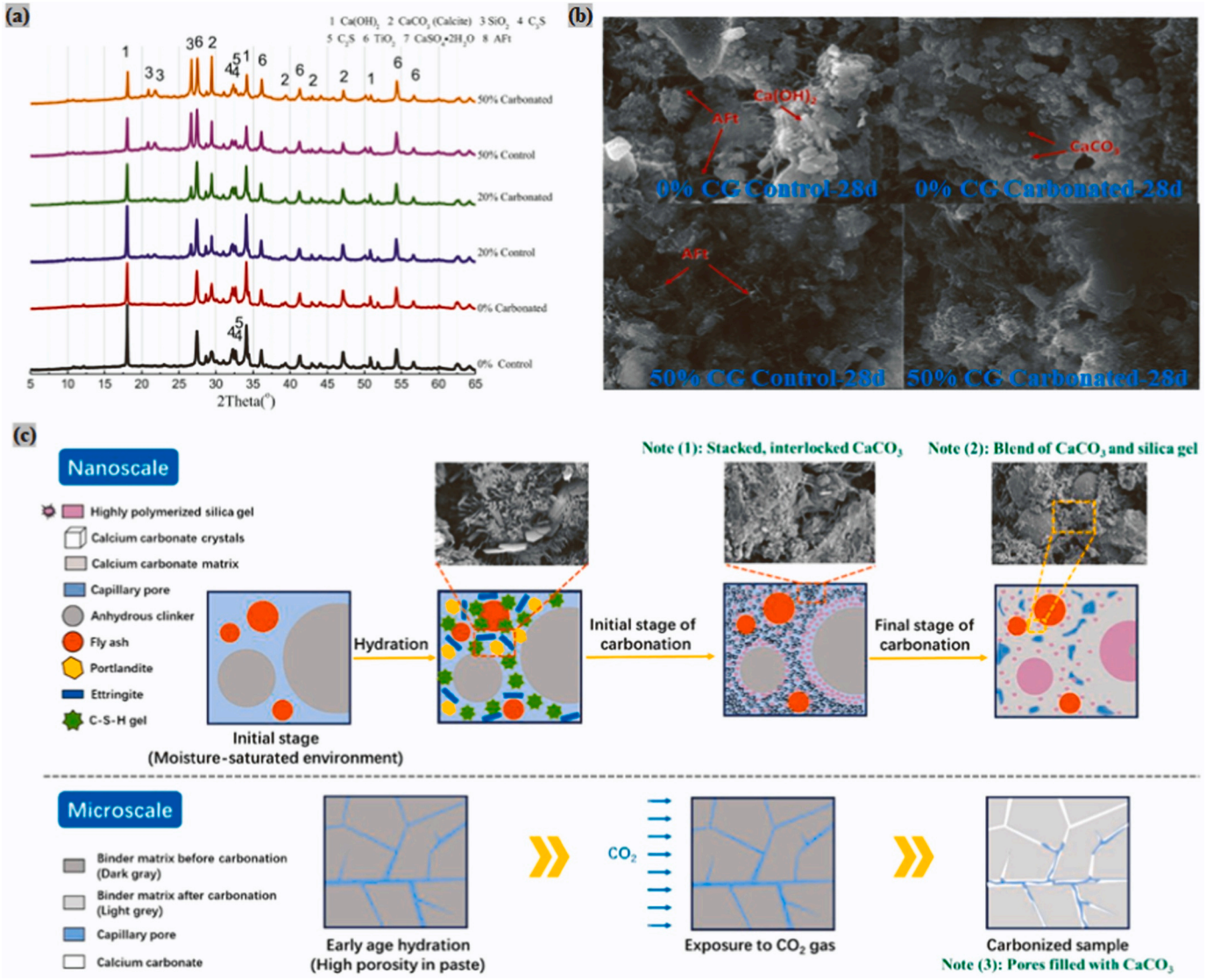

Fig. 17. The microstructure of CSBW with carbonation curing (a) XRD, (b) SEM and (c) Schematic diagram [169,172].

Analysis of XRD patterns and SEM images of PC-CG paste specimens before and after carbonation reveals a decrease in $Ca(OH)_2$ peak intensity and an increase in $CaCO_3$ peak intensity (Fig. 17a). This transformation of AFt and $Ca(OH)_2$ into substantial amounts of $CaCO_3$ effectively fills the original pores, enhancing structural density. Additionally, $Ca(OH)_2$ is prone to dissolution under flowing water, but the denser Ca-modified shell layer formed by carbonation effectively mitigates dissolution erosion [172] (Fig. 17b). Overall, carbonation curing enhances CBSW concrete performance by forming a dense, interlocking $CaCO_3$ protective layer on the surface of hydration products and CBSW, promoting strong bonding between C-S-H gel and $CaCO_3$ crystals, and filling capillary pores with $CaCO_3$ (Fig. 17c).

5.3. The carbon emissions assessment on the life cycle of CBSW concrete

Carbon emissions are critical indicators for assessing environmental impacts and are extensively used in environmental impact studies [173]. Carbon emission factors express the carbon emissions per unit of energy consumed during production activities. Carbon emissions can be estimated as the product of input energy consumption and emission factors according to different production activity segments (Eq. 1) [174].

$$\text{Emissions} = \sum_1^n A_i \times EF_i \times (1 - ER) \quad (1)$$

where Emissions refers to the carbon emissions, A_i is the i_{th} activity level, EF_i is the carbon emission factor for the i_{th} activity, and ER is the abatement rate (%).

As shown in Fig. 18, a comparison of carbon emissions during the three stages of production—preparation and transportation of raw materials, concrete placement, and curing—between traditional and CBSW concrete is conducted using a cradle-to-gate system boundary [175, 176]. Carbon emissions from concrete primarily originate from the raw materials. Generally, the more raw materials required to prepare high-strength concrete, the higher the carbon emissions. Although the GB/T 51366–2019 standard specifies carbon emission factors of 295 and 385 $kgCO_2e/m^3$ for C30 and C50 concrete, respectively, literature analysis indicates that the CO_2 emissions of concrete vary significantly depending on the types of raw materials and mix ratios, for example, the carbon emissions of lime are significantly higher than those of other raw materials. Therefore, increasing the proportion of lime in the mix can substantially raise the CO_2 emissions of concrete. As shown in Fig. 18, the CO_2 emissions for C30, C40, and C50 are similar [177–179]. It is only at C70 and C80 that concrete's carbon emissions increase substantially. And as shown in the figure, utilizing alkali activation technology can significantly reduce the carbon emissions of concrete [180–182]. Since the carbon emissions from fly ash production are lower than those from cement production, replacing cement with fly ash in concrete preparation reduces carbon emissions throughout its life cycle [183–185]. The production of coal gangue aggregate requires only simple crushing, resulting in lower total emissions [186,187]. Additionally, increased transportation distances contribute to higher carbon emissions. Different life cycle databases identify varying carbon emission factors, leading to differences in estimated carbon emissions.

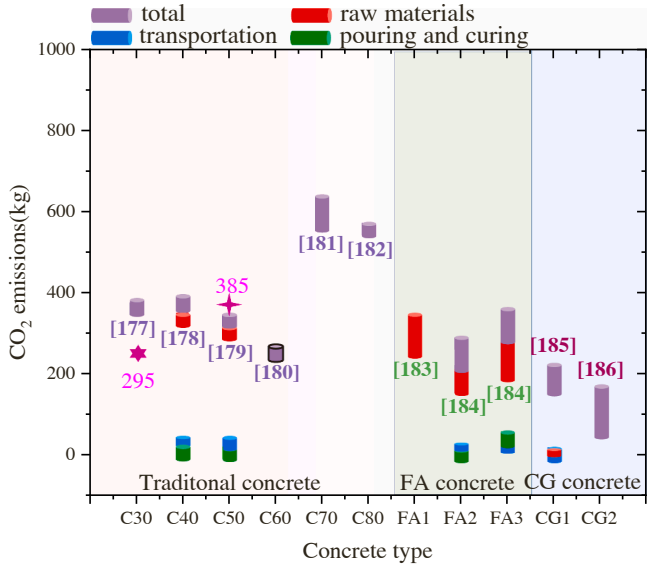

Fig. 18. The carbon emissions assessment of concrete [177–187](FA1 represents 15–35 % FA content, FA2 represents 30–50 % FA content, FA3 represents 100 % FA content ; CG1 represents 10–20 % CG content, CG2 represents 15–60 % FA content).

6. Conclusions and prospects

6.1. Conclusions

Utilizing typical coal-based solid waste (CBSW) in building materials presents a dual benefit for sustainable waste management and carbon reduction. This paper reviews the differences in properties among typical CBSWs, the impact of pretreatment methods on performance, the effects of CBSW content and properties on concrete performance mechanisms, and the influence of carbonation curing parameters on CO2 absorption and CBSW concrete performance. The findings offer valuable insights for researchers in environmental science, building materials, the chemical industry, and energy sectors. The key conclusions are as follows:

1) The inert SiO_2 and Al_2O_3 in coal gangue (CG) have weak binding abilities, necessitating calcination to enhance activity. Fly ash (FA) contains non-calcium oxides with strong hydration activity. The high residual carbon and impurity content in coal gasification slag (CGS) results in its low comprehensive utilization rate.

2) Common activation methods for CG and CGS include crushing and impurity removal. Mechanical grinding enhances CG activity by increasing particle specific surface area, reducing size, and enriching surface aluminum. CGS achieves residual carbon capture through gravity concentration and foam flotation. Thermal activation significantly enhances CG activity, peaking at approximately 800°C. CBSW undergoes dissolution, depolymerization, and condensation stages to break Si-O-Si and Al-O-Al covalent bonds, increasing three-dimensional polymeric aluminum salts and achieving chemical activation.

3) Due to its loose structure, numerous pores, and flaky particles, CG exhibits significant performance fluctuations. Cement slurry coatings significantly improve concrete's mechanical properties. Techniques such as CO_2 curing, microbially induced carbonate precipitation, and nano-silica spraying effectively enhance concrete performance. FA's filling and nucleation effects are effective in filling concrete pores and improving structural compactness. Due to its high carbon content and particle size variability, the optimal CGS content in concrete usually does not exceed 30 %. Addressing the carbon content issue in CGS is a future research priority in building materials.

4) CO_2 concentration, carbonation pressure, carbonation time, carbonation temperature, and pretreatment methods significantly affect CO_2 absorption rate and amount. Carbonation curing compensates for strength loss from cement replacement by forming carbonates that fill surface pores and create a dense microstructure. The coupling effect between CBSW and carbonation enhances concrete durability. Utilizing different CBSW concrete mix ratios based on application needs can contribute to sustainable development.

6.2. Prospects

1)Fully activating the potential of CBSW is challenging when used alone. Elucidating synergistic mechanisms among multiple solid wastes and determining optimal proportions for various applications are

essential for achieving high-volume utilization and complementary performance advantages.

2) Studies on the combination of carbonation curing and CBSW concrete are scarce, likely due to inherent defects in many coal-based solid wastes. Addressing these challenges requires selecting appropriate modification methods tailored to specific CBSW characteristics for functional utilization. Developing new technologies to enhance the utilization of coal-based solid waste is critical.

3) To standardize carbon emissions from building materials, extensive research on carbon emission factors has been conducted. However, most studies focus on common building materials. Establishing a comprehensive database of carbon emission factors for CBSW concrete is urgently needed to address this research gap.

Future efforts should focus on utilizing low-carbon raw materials, optimizing concrete mix ratios, and establishing standards and specifications for the entire process—from solid waste raw material selection, production, grading, and storage to application. This approach will facilitate the synergistic use of multi-solid waste resources and reduce carbon emissions during production, offering broad application prospects and significant social benefits.

CRediT authorship contribution statement

ling qin: Resources, Methodology. **Shanbin Xue:** Project administration, Methodology. **Jiuwen bao:** Supervision, Software, Resources. **shipeng xu:** Project administration, Methodology. **peng zhang:** Project administration, Methodology, Investigation. **qiang song:** Funding acquisition, Formal analysis, Data curation, Conceptualization. **Yingjie Zou:** Investigation, Funding acquisition, Formal analysis, Data curation. **changsha liu:** Formal analysis. **liang lin:** Data curation. **hui wang:** Methodology.

Declaration of Competing Interest

The authors declare that they have no known competing financial interests or personal relationships that could have appeared to influence the work reported in this paper.

Data availability

Data will be made available on request.

Acknowledgements

This work is supported by National Natural Science Foundation of China (52341803, 42102214, 51922052, 51778309), National Key Research and Development Program of China (2021YFB2600704), Project for Excellent Youth Foundation of the Innovation Teacher Team, Shandong (2022KJ310), Youth Foundation of Shandong Natural Science Foundation of China (ZR2020QE138, ZR2020QE249, ZR2023MD036), Xi'an University of Science and Technology, State Key Laboratory of Coal Resources in Western China (SKLCRKF20-15), Key Laboratory of Coal Resources Exploration and Comprehensive Utilization, Ministry of Natural Resources (KF2021-8).

References

[1] N. Ankur, N. Singh, Performance of cement mortars and concretes containing coal bottom ash: a comprehensive review, Renew. Sustain. Energy Rev. 149 (2021) 111361.
[2] Q. Song, H.Y. Zhao, Q.X. Ma, L. Yang, L. Ma, Y. Wu, et al., Catalytic upgrading of coal volatiles with Fe_2O_3 and hematite by TG-FTIR and Py-GC/MS, Fuel 313 (2022) 122667.
[3] J.Y. Li, J.M. Wang, Comprehensive utilization and environmental risks of coal gangue: a review, J. Clean. Prod. 239 (2019) 117946.
[4] M.J. Moghadam, R. Ajalloeian, A. Hajiannia, Preparation and application of alkali-activated materials based on waste glass and coal gangue: a review, Constr. Build. Mater. 221 (2019) 84–98.
[5] Y.L. Zhang, T.C. Ling, Reactivity activation of waste coal gangue and its impact on the properties of cement-based materials – a review, Constr. Build. Mater. 234 (2020) 117424, https://doi.org/10.1016/j.conbuildmat.2019.117424.
[6] C.C. Zhou, G.J. Liu, T. Fang, R.Y. Sun, D. Wu, Leaching characteristic and environmental implication of rejection rocks from Huainan Coalfield, Anhui Province, China, J. Geochem Explor 143 (2014) 54–61, https://doi.org/10.1016/j, gexplo.2014.03.010.
[7] Q. Tang, L.Y. Li, S. Zhang, L.G. Zheng, C.H. Miao, Characterization of heavy metals in coal gangue-reclaimed soils from a coal mining area, J. Geochem Explor 186 (2018) 1–11, https://doi.org/10.1016/j.gexplo.2017.11.018.
[8] Y.Z. Sun, J.S. Fan, P. Qin, H.Y. Niu, Pollution extents of organic substances from a coal gangue dump of Jiulong Coal Mine, China, Environ. Geochem Hlth 31 (2009) 81–89, https://doi.org/10.1007/s10653-008-9158-9.
[9] X.W. Wang, N.N. Zhong, D.M. Hu, Z.Z. Liu, Z.H. Zhang, Polycyclic aromatic hydrocarbon (PAHs) pollutants in groundwater from coal gangue stack area: characteristics and origin, Water Sci. Technol. 59 (2009) 1043–1051, https://doi.org/10.2166/wst.2009.050.
[10] C. Cui, S. Jiang, H. Shao, W. Zhang, K. Wang, Z. Wu, Experimental study on thermo-responsive inhibitors inhibiting coal spontaneous combustion, Fuel Process Technol. 175 (2018) 113–122.
[11] J. Wang, Y. Zhang, S. Xue, J. Wu, Y. Tang, L. Chang, Assessment of spontaneous combustion status of coal based on relationships between oxygen consumption and gaseous product emissions, Fuel Process Technol. 179 (2018) 60–71.
[12] J.W. Bao, Y.W. Wang, H.R. Zhang, S.G. Li, P. Zhang, L. Qin, Q. Song, Effect of loading-induced damage on chloride ingress behavior of recycled aggregate concrete: a comprehensive review, Cem. Concr. Comp. 141 (2023) 105123.
[13] H. Wu, Q.B. Wen, L.M. Hu, M. Gong, Z.L. Tang, Feasibility study on the application of coal gangue as landfill liner material, Waste Manag. 63 (2017) 161–171.
[14] R.S. Krishna, F. Shaikh, J. Mishra, G. Lazorenko, A. Kasprzhitskii, Mine tailings-based geopolymers: properties, applications and industrial prospects, Ceram. Int. 47 (2021) 17826–17843, https://doi.org/10.1016/j.ceramint.2021.03.180.
[15] J. Deng, B. Li, Y. Xiao, C.P. Wang, L.W. Bin, C.M. Shu, Combustion properties of coal gangue using thermogravimetry–Fourier transform infrared spectroscopy, Appl. Therm. Eng. 116 (2017) 244–252.
[16] Y.Y. Zhang, Y.X. Guo, F.Q. Cheng, K.Z. Yan, Y. Cao, Investigation of combustion characteristics and kinetics of coal gangue with different feedstock properties by thermogravimetric analysis, Thermochim. Acta 614 (2015) 137–148.
[17] C.F. Liang, H.W. Ma, Y.Q. Pan, Z.M. Ma, Z.H. Duan, Z.H. He, Chloride permeability and the caused steel corrosion in the concrete with carbonated recycled aggregate, Constr. Build. Mater. 218 (2019) 506–518.
[18] Y.Z. Wang, Y. Tan, Y.C. Wang, C.X. Li, Mechanical properties and chloride permeability of green concrete mixed with fly ash and coal gangue, Constr. Build. Mater. 233 (2020) 117166.
[19] Y. Wang, L. Burris, R.D. Hooton, C.R. Shearer, P. Suraneni, Effects of unconventional fly ashes on cementitious paste properties, Cem. Concr. Comp. 125 (2022) 104291.
[20] X.B. Zhu, W.H. Gong, W. Li, X.Y. Bai, C.X. Zhang, Reclamation of waste coal gangue activated by Stenotrophomonas maltophilia for mine soil improvement: solubilizing behavior of bacteria on nutrient elements, J. Environ. Manag. 320 (2022) 115865, https://doi.org/10.1016/j.jenvman.2022.115865.
[21] R. Kaur, D. Goyal, Mineralogical comparison of coal fly ash with soil for use in agriculture, J. Mater. Cycles Waste 18 (2016) 186–200, https://doi.org/10.1007/s10163-014-0323-1.
[22] H. Li, F. Zheng, J. Wang, J.M. Zhou, X.H. Huang, L. Chen, P.F. Hu, J.M. Gao, Q. Zheng, S. Bashir, J.L. Liu, Facile preparation of zeolite-activated carbon composite from coal gangue with enhanced adsorption performance, Chem. Eng. J. 390 (2020) 124513.
[23] S. Pyo, S.Y. Abate, H.K. Kim, Abrasion resistance of ultra high performance concrete incorporating coarser aggregate, Constr. Build. Mater. 165 (2018) 11–16.
[24] J. Beata, V.K. Andriy, B. Mark, H. Patrick, The structural and surface properties of natural and modified coal gangue, J. Environ. Manag. 190 (2017) 80–90, https://doi.org/10.1016/j.jenvman.2016.12.055.
[25] L. Qin, X.J. Gao, Properties of coal gangue-Portland cement mixture with carbonation, Fuel 245 (2019) 1–12.
[26] L. Dong, X.X. Liang, Q. Song, G.W. Gao, L.H. Song, Y.F. Shu, X.Q. Shu, Study on Al_2O_3 extraction from activated coal gangue under different calcination atmospheres, J. Therm. Sci. 26 (2017) 570–576.
[27] X. Yang, Y. Zhang, Z. Li, Embankment displacement PLAXIS simulation and microstructural behavior of treated-coal gangue, Minerals 10 (3) (2020) 218, https://doi.org/10.3390/min10030218.
[28] G.C. Long, L.H. Li, W.G. Li, K.L. Ma, W.K. Dong, C.N. Bai, J.L. Zhou, Enhanced mechanical properties and durability of coal gangue reinforced cement-soil mixture for foundation treatments, J. Clean. Prod. 231 (2019) 468–482.
[29] C.L. Liu, J.P. Xia, H. Fan, W.L. Li, G.Y. Zheng, G. Ma, Y.F. Liang, Ti leaching differences during acid leaching of coal gangue based on different thermal fields, Waste Manag. 101 (2020) 66–73.
[30] N. Koshy, K. Dondrob, L.M. Hu, Q.B. Wen, J.N. Meegoda, Synthesis and characterization of geopolymers derived from coal gangue, fly ash and red mud, Constr. Build. Mater. 206 (2019) 287–296.
[31] Z. Li, Y. Gao, J. Zhang, C. Zhang, J.P. Chen, C. Liu, Effect of particle size and thermal activation on the coal gangue based geopolymer, Mater. Chem. Phys. 267 (2021) 124657, https://doi.org/10.1016/j.matchemphys.2021.124657.
[32] S.Y. Ouyang, Y.L. Huang, H.D. Gao, Y.C. Guo, L.W. Wu, J.M. Li, Study on the distribution characteristics and ecological risk of heavy metal elements in coal

gangue taken from 25 mining areas of China, Environ. Sci. Pollut. R 29 (2022) 48285–48300, https://doi.org/10.1007/s11356-022-19238-3.
[33] H.D. Gao, Y.L. Huang, W. Li, J.M. Li, S.Y. Ouyang, T.Q. Song, F.Y. Lv, W. Zhai, K. Ma, Explanation of heavy metal pollution in coal mines of china from the perspective of coal gangue geochemical characteristics, Environ. Sci. Pollut. R 28 (2021) 1–11, https://doi.org/10.1007/s11356-021-14766-w.
[34] A. Bhatt, S. Priyadarshini, A. Mohanakrishnan, A. Abri, M. Sttler, S. Techapaphawit, Physical, chemical, and geotechnical properties of coal fly ash: a global review, Case Stdu Constr. Mat. 11 (2019) e00263, https://doi.org/10.1016/j.cscm.2019.e00263.
[35] N.N. Deepak, D.P. Yogesh, Performance of coal bottom ash concrete at elevated temperatures, Mater. Today Proc. 65 (2022) 883–888, https://doi.org/10.1016/j, matpr.2022.03.519.
[36] H. Hamada, A. Alattar, B. Tayeh, F. Yahaya, A. Adesina, Sustainable application of coal bottom ash as fine aggregates in concrete: a comprehensive review, Case Stdu Constr. Mat. 16 (2022) e01109.
[37] P. Yang, Y.L. Suo, L. Liu, H.S. Qu, G. Xie, C.X. Zhang, S.C. Deng, Study on the curing mechanism of cemented backfill materials prepared from sodium sulfate modified coal gasification slag, J. Build. Eng. 62 (2022) 105318.
[38] C. Patricia, Status of flue gas desulphurisation (FGD) systems from coal-fired power plants: overview of the physic-chemical control processes of wet limestone FGDs, Fuel 144 (2015) 274–286.
[39] Y.C. Dong, S.B. Mao, F.Q. Guo, R. Shu, J.M. Bai, L. Qian, Y.H. Bai, Coal gasification fine slags: Investigation of the potential as both microwave adsorbers and catalysts in microwave-induced biomass pyrolysis applications, Energy 238 (2022) 121867.
[40] J.H. Zhao, D.M. Wang, S.C. Liao, Effect of mechanical grinding on physical and chemical characteristics of circulating fluidized bed fly ash from coal gangue power plant, Constr. Build. Mater. 101 (2015) 851–860.
[41] W.Q. Zhang, C.W. Dong, P. Huang, Q. Sun, M. Li, H. Chai, Experimental study on the characteristics of activated coal gangue and coal gangue-based geopolymer, Energies 13 (2020) 2504.
[42] Z.L. Zhou, S. Zhang, Z.Y. Gao, X. Cai, H. Li, Multifractal characterization of gangue particle size distribution structure during ball milling process, Powder Technol. 412 (2022) 117970.
[43] Y.X. Guo, K.Z. Yan, L. Cui, F.Q. Cheng, Improved extraction of alumina from coal gangue by surface mechanically grinding modification, Powder Technol. 302 (2016) 33–41.
[44] W. Yu, H.L. Zhang, X.B. Wang, Z.U. Rahman, Z.C. Shi, Y.H. Bai, G.S. Wang, Y. Q. Chen, J.J. Wang, L.J. Liu, Enrichment of residual carbon from coal gasification fine slag by spiral separator, J. Environ. Manag. 315 (2022) 115149, https://doi.org/10.1016/j.jenvman.2022.115149.
[45] L. Yang, D.L. Li, Z.N. Zhu, M. Xu, X.K. Yang, H.J. Zhang, Effect of the intensification of preconditioning on the separation of unburned carbon from coal fly ash, Fuel 242 (2019) 174–183.
[46] D. Shi, J.B. Zhang, X.J. Hou, S.P. Li, H.Q. Li, F.Y. He, Adsorption mechanism of a new combined collector (PS-1) on unburned carbon in gasification slag, Sci. Total Environ. 818 (2022) 151856.
[47] Z.H. Xue, L.P. Dong, M.Q. Fan, H.L. Yang, A. Liu, Z.H. Li, W.R. Bao, J.C. Wang, P. P. Fan, Ehanced flotation mechanism of coal gasification fine slag with composite collectors, Colloid Surf. A 641 (2022) 128593, https://doi.org/10.1016/j.colsurfa.2022.128593.
[48] A.M. Rashad, Metakaolin as cementitious material: history, scours, production and composition – A comprehensive overview, Constr. Build. Mater. 41 (2013) 303–318.
[49] A. Shvarzman, K. Kovler, G.S. Grader, The effect of dehydroxylation/amorphization degree on pozzolanic activity of kaolinite, Cem. Concr. Res. 33 (2003) 405–416.
[50] Y.B. Zhao, C.Q. Yang, K.F. Li, F. Qu, C.Y. Yan, Z.R. Wu, Toward understanding the activation and hydration mechanisms of composite activated coal gangue geopolymer, Constr. Build. Mater. 319 (2022) 125999.
[51] A.H. Muhammad, F.H. Mohd, N.A. Farud, Microwave torrefaction for viable fuel production: a review on theory, affecting factors, potential and challenges, Fuel 253 (2019) 512–526.
[52] S.L. Zhong, M.S. Zhong, Q. Su, Study of mechanism of kaolin sintered by microwave heating, Acta Sci. Nat. Univ. Sunyatseni. 3 (2005) 71–74.
[53] X. Guan, J.X. Chen, M.Y. Zhu, J. Gao, Performance of microwave-activated coal gangue powder as auxiliary cementitious material, J. Mater. Res. Technol. 14 (2021) 2799–2811, https://doi.org/10.1016/j.jmrt.2021.08.106.
[54] B.J. Frasson, R.C. Pinto, J.C. Rocha, Influence of different sources of coal gangue used as aluminosilicate powder on the mechanical properties and microstructure of alkali-activated cement, Mater. Constr. 69 (2019) 199, https://doi.org/10.3989/mc.2019.12618.
[55] C.J. Shi, B. Qu, J.L. Provis, Recent progress in low-carbon binders, Cem. Concr. Res. 122 (2019) 227–250.
[56] A. Fernández-Jiménez, A. Palomo, M. Criado, Microstructure development of alkali-activated fly ash cement: a descriptive model, Cem. Concr. Res. 35 (2005) 1204–1209.
[57] A. Fernández-Jiménez, A. Palomo, I. Sobrados, J. Sanz, The role played by the reactive alumina content in the alkaline activation of fly ashes, Micro Mesopor Mat. 91 (2006) 111–119, https://doi.org/10.1016/j.micromeso.2005.11.015.
[58] A. Palomo, S. Alonso, A. Fernández-Jiménez, I. Sobrados, J. Sanz, Alkaline activation of fly ashes: NMR study of the reaction products, J. Am. Ceram. Soc. 87 (2004) 1141–1145, https://doi.org/10.1111/j.1551-2916.2004.01141.x.
[59] A. Saedi, A. Jamshidi-Zanjani, D.A. Khodadadi, A review on different methods of activating tailings to improve their cementitious property as cemented paste and reusability, J. Environ. Manag. 270 (2020) 110881, https://doi.org/10.1016/j.jenvman. 2020.110881.
[60] A.O. Purdon, The action of alkalis on blast furnace slag, J. Soc. Chem. Ind. 59 (1940) 191–202.
[61] S.M. Park, J.G. Jang, N.K. Lee, H.K. Lee, Physicochemical properties of binder gel in alkali-activated fly ash/slag exposed to high temperatures, Cem. Concr. Res. 89 (2016) 72–79.
[62] C. Yi, H.Q. Ma, H. Chen, J.X. Wang, J. Shi, Z.H. Li, et al., Preparation and characterization of coal gangue geopolymers, Constr. Build. Mater. 187 (2018) 318–326.
[63] J.Y. Han, X.Y. Song, Z.H. Gao, Excitation effect of soluble glass on composite system with calcined coal gangue and slag, Appl. Mech. Mater. 174-177 (2012) 30–34, https://doi.10.4028/www.scientific,net/AMM.174-177.30.
[64] R.C. Han, X.N. Guo, J.F. Guan, X.H. Yao, Y. Hao, Activation mechanism of coal gangue and its impact on the properties of geopolymers: a review, Polymers 14 (2022) 3861.
[65] J. Yang, H. Bai, X.Y. He, J.Y. Zeng, Y. Su, X.D. Wang, et al., Performances and microstructure of one-part fly ash geopolymer activated by calcium carbide slag and sodium metasilicate powder, Constr. Build. Mater. 367 (2023) 130303.
[66] H.Y. Leong, D.E.L. Ong, J.G. Sanjayan, A. Nazari, The effect of different Na_2O and K2O ratios of alkali activator on compressive strength of fly ash based-geopolymer, Constr. Build. Mater. 106 (2016) 500–511.
[67] S. Alahrache, F. Winnefeld, J.B. Champenois, F. Hesselbarth, B. Lothenbach, Chemical activation of hybrid binders based on siliceous fly ash and Portland cement, Cem. Concr. Comp. 66 (2016) 10–23.
[68] Y.C. Chen, X. Zhou, S. Wan, R. Zheng, J. Tong, H.B. Hou, T.S. Wang, Synthesis and characterization of geopolymer composites based on gasification coal fly ash and steel slag, Constr. Build. Mater. 211 (2019) 646–658.
[69] Z.Z. Li, Y.Y. Zhang, H.Y. Zhao, H.X. Chen, R. He, Structure characteristics and composition of hydration products of coal gasification slag mixed cement and lime, Constr. Build. Mater. 213 (2019) 265–274.
[70] Y. Lee, S.K. Bang, Study on a nano-microstructure and properties of geopolymer by recycling integrated gasification combined cycle coal ash slag, J. Nanosci. Nanotechnol. 19 (2019) 2193–2197.
[71] S.H. Zhang, M.Y. Cao, K.F. Zhang, J. Yuan, Y. Wang, Wrapped coal gangue aggregate enhancement ITZ and mechanical property of concrete suitable for large-scale industrial use, J. Build. Eng. 72 (2023) 106649.
[72] Q. Xu, Y.Z. Zhang, H.Q. Liu, M. Zhou, Q.H. Wang, H.F. Lin, Effect of spontaneous-combustion coal gangue aggregate on axial performance of square concrete-filled steel tube stub columns, Structures 44 (2022) 216–235.
[73] T.R. Zhang, Y.Z. Zhang, Q.H. Wang, A.K. Aganyira, Y.F. Fang, Experimental study and machine learning prediction on compressive strength of spontaneous-combustion coal gangue aggregate concrete, J. Build. Eng. 71 (2023) 106518.
[74] W.C. Gao, X.L. Zhang, G.Z. Du, Y.P. Ma, J.B. Fan, Y. Geng, et al., Shrinkage model for concrete incorporating coal gangue coarse and fine aggregates, J. Build. Eng. 80 (2023) 107865.
[75] Y.G. Mao, J.H. Liu, C.J. Shi, Autogenous shrinkage and drying shrinkage of recycled aggregate concrete: a review, J. Clean. Prod. 295 (2021) 126435.
[76] L. Liu, D.X. Xuan, A.O. Sojobi, S.H. Liu, C.S. Poon, Efficiencies of carbonation and nano silica treatment methods in enhancing the performance of recycled aggregate concrete, Constr. Build. Mater. 308 (2021) 125080.
[77] S.C. Kou, B.J. Zhan, C.S. Poon, Use of a CO_2 curing step to improve the properties of concrete prepared with recycled aggregates, Cem. Concr. Compos 45 (2014) 22–28.
[78] C.H. Feng, B.W. Cui, Y.H. Huang, H. Guo, W.Y. Zhang, J.P. Zhu, Enhancement technologies of recycled aggregate – Enhancement mechanism, influencing factors, improvement effects, technical difficulties, life cycle assessment, Constr. Build. Mater. 317 (2022) 126168.
[79] X. Guan, J.X. Chen, M.Y. Zhu, J. Gao, Performance of microwave-activated coal gangue powder as auxiliary cementitious material, J. Mater. Res. Technol. 14 (2021) 2799–2811.
[80] J.F. Zhang, H.Y. Han, L. Wang, Pozzolanic activity experimental dataset of calcined coal gangue, Data Brief. 51 (2023) 109802.
[81] W. Sun, H.D. Yan, B.G. Zhang, Analysis of mechanism on water-reducing effect of fine ground slag, high-calcium fly ash, and low-calcium fly ash, Cem. Concr. Res. 33 (2003) 1119–1125.
[82] C.Y. Lee, H.K. Lee, K.M. Lee, Strength and microstructural characteristics of chemically activated fly ash-cement systems, Cem. Concr. Res. 33 (2003) 425–431.
[83] D. Dong, Y.B. Huang, Y. Pei, X.Y. Zhang, N. Cui, P.Q. Zhao, P.K. Hou, L.C. Lu, Effect of spherical silica fume and fly ash on the rheological property, fluidity, setting time, compressive strength, water resistance and drying shrinkage of magnesium ammonium phosphate cement, J. Build. Eng. 63 (2023) 105484.
[84] L.J. Su, G.S. Fu, B. Liang, Q. Sun, X.D. Zhang, Z. Shen, Working performance and microscopic mechanistic analyses of municipal solid waste incineration (MSWI) fly ash-based self-foaming filling materials, Constr. Build. Mater. 361 (2022) 129647.
[85] S.L. Zhang, X.Q. Qi, S.Y. Guo, L. Zhang, J. Ren, A systematic research on foamed concrete: the effects of foam content, fly ash, slag, silica fume and water-to-binder ratio, Constr. Build. Mater. 339 (2022) 127683.
[86] R. Rumman, M.R. Kamal, A. Bediwy, M.S. Alam, Partially burnt wood fly ash characterization and its application in low-carbon mortar and concrete, Constr. Build. Mater. 402 (2023) 132946.
[87] L.S. Zhang, Z.D. Chen, R. Chen, S.J. Zhu, H.N. Lin, P. Tai, Compressive strength of fly ash based geopolymer utilizing waste completely decomposed granite, Case Stud. Constr. Mat. 19 (2023) e02667.

[88] X. Zhang, X.P. Feng, Z.P. Wang, J.C. Jian, S. Chen, W. Luo, C. Zhang, Experimental study on the physico-mechanical properties and microstructure of foam concrete mixed with coal gangue, Constr. Build. Mater. 359 (2023) 129428.
[89] T. Wang, X.J. Gao, Y.L. Li, Y.H. Liu, An orthogonal experimental study on the influence of steam-curing on mechanical properties of foam concrete with fly ash, Case Stud. Constr. Mat. 20 (2024) e02665.
[90] J.W. Bao, J.N. Wei, P. Zhang, Z.J. Zhuang, T.J. Zhao, Experimental and theoretical investigation of chloride ingress into concrete exposed to real marine environment, Cem. Concr. Comp. 130 (2022) 104511.
[91] A.G. Vayghan, J.R. Wright, F. Rajabipour, An extended chemical index model to predict the fly ash dosage necessary for mitigating alkali–silica reaction in concrete, Cem. Concr. Res. 82 (2016) 1–10.
[92] Y.Y. Wang, Z.H. Shui, X. Gao, R. Yu, Y. Huang, S.K. Chen, Understanding the chloride binding and diffusion behaviors of marine concrete based on Portland limestone cement-alumina enriched pozzolans, Constr. Build. Mater. 198 (2019) 207–217.
[93] M.H. Shehata, M.D.A. Thomas, R.F. Bleszynski, The effects of fly ash composition on the chemistry of pore solution in hydrated cement pastes, Cem. Concr. Res. 29 (1999) 1915–1920.
[94] M. Teymouri, M. Shakour, Chloride desorption mechanisms of cement pastes containing fly ash, Constr. Build. Mater. 370 (2023) 130667.
[95] B. Lothenbach, K. Scrivener, R.D. Hooton, Supplementary cementitious materials, Cem. Concr. Res 41 (2011) 1244–1256.
[96] W.H. Liu, X.Y. Liu, L. Zhang, Y.F. Wan, H. Li, X.D. Jiao, Rheology, mechanics, microstructure and durability of low-carbon cementitious materials based on circulating fluidized bed fly ash: a comprehensive review, Constr. Build. Mater. 411 (2024) 134688.
[97] C.F. Liang, B.H. Pan, Z.M. Ma, Z.H. He, Z.H. Duan, Utilization of CO_2 curing to enhance the properties of recycled aggregate and prepared concrete: a review, Cem. Concr. Comp. 105 (2020) 103446.
[98] Q. Song, J.W. Bao, S.B. Xue, P. Zhang, S.N. Mu, Collaborative disposal of multisource solid waste: Influence of an admixture on the properties, pore structure and durability of foam concrete, J. Mater. Res. Technol. 14 (2021) 1778–1790.
[99] S.H. Zhang, B.F. Chen, B. Tian, X.C. Lu, B.B. Xiong, Effect of fly ash content on the microstructure and strength of concrete under freeze–thaw condition, Buildings 12 (2022) 2113.
[100] K.Z. Fang, D.J. Zhang, D.M. Wang, Z. Liu, M. Zhang, S. Zhang, The impact of coal gasification slag powder on fluidity, rheology and viscoelasticity properties of fresh cement paste, J. Build. Eng. 69 (2023) 106237.
[101] Y. Tian, Z.L. Xie, K.W. Xue, Q. Yuan, C.H. Yang, B. Fu, X.H. Zhu, The role of coal gasification slag in cement paste with and without polycarboxylate superplasticizer and its rheology, Constr. Build. Mater. 373 (2023) 130852.
[102] J.C. Xiang, J.P. Qiu, Y.Q. Zhao, P.K. Zheng, H.N. Peng, X.C. Fei, Rheology, mechanical properties, and hydration of synergistically activated coal gasification slag with three typical solid wastes, Cem. Concr. Comp. 147 (2024) 105418.
[103] B. Fu, Z.Y. Chen, D.Z. Wang, N. Li, Investigation on the utilization of coal gasification slag in Portland cement: reaction kinetics and microstructure, Constr. Build. Mater. 323 (2023) 126587.
[104] C.S. Chen, S. Shenoy, Y.H. Pan, K. Sasaki, Q.Z. Tian, H.J. Zhang, Mechanical activation of coal gasification slag for one-part geopolymer synthesis by alkali fusion and component additive method, Constr. Build. Mater. 411 (2024) 134585.
[105] G. Xie, L. Liu, Y.L. Suo, P. Yang, C.X. Zhang, H.S. Qu, Y. Lv, Hydration mechanism of calcium chloride modified coal gasification slag-based backfill materials, Process Saf. Environ. 182 (2024) 127–138.
[106] P. Yang, L. Liu, T.L. Suo, G. Xie, W.J. Sun, C.X. Zhang, Physical-chemical coupling excitation of low activity coal gasification slag solid waste and its application as a backfill cementitious material, Constr. Build. Mater. 401 (2023) 132973.
[107] F. Wu, H. Li, K. Yang, Effects of mechanical activation on physical and chemical characteristics of coal-gasification slag, Coatings 11 (2021) 902.
[108] X.L. Zhu, Z.H. Guo, W. Yang, W.J. Song, Durability of concrete with coal gasification slag and coal gangue powder, Front Mater. 8 (2021) 791178, https://doi.org/10.3389/fmats.2021.791178.
[109] H.W. Li, Q.K. Nie, C. Wang, G.H. Wang, L. Zhang, L.L. Yuan, Durability investigation of fractured coal-gasified ash slag concrete eroded by sulfate and chlorine salts, Case Stud. Constr. Mat. 20 (2024) e02745.
[110] Y.X. Guo, W.Y. Hu, G.R. Feng, Y.H. Zhao, C.Q. Li, X.X. Wang, J.H. Ma, Study on the excitation effect and mechanism of coal gasification slag based on solid waste, Powder Technol. 434 (2024) 119460.
[111] J.P. Won, H.H. Kim, S.J. Lee, S.J. Choi, Carbon reduction of precast concrete under the marine environment, Constr. Build. Mater. 74 (2015) 118–123.
[112] N. Shehata, E.T. Sayed, M.A. Abdelkareem, Recent progress in environmentally friendly geopolymers: a review, Sci. Total Environ. 762 (2021) 143166.
[113] S. Monkman, M. Macdonald, On carbon dioxide utilization as a means to improve the sustainability of ready-mixed concrete, J. Clean. Prod. 167 (2017) 365–375.
[114] M. Mastali, Z. Abdollahnejad, F. Pacheco-Torgal, Performance of waste based alkaline mortars submitted to accelerated carbon dioxide curing, Resour. Conserv Recyl. 129 (2018) 12–19.
[115] S.H. Bong, M. Xia, B. Nematollahi, C.J. Shi, Ambient temperature cured 'just-add-water' geopolymer for 3D concrete printing applications, Cem. Concr. Comp. 121 (2021) 104060.
[116] J. Jeong, T. Hong, C. Ji, J. Kim, M. Lee, K. Jeong, S. Lee, An integrated evaluation of productivity, cost and CO_2 emission between prefabricated and conventional columns, J. Clean. Prod. 142 (2017) 2393–2406.
[117] Maries A. The activation of Portland cement by carbon dioxide, in: Proceedings of Conference in Cement and Concrete Science, Oxford, UK, 1985.
[118] M.F. Bertos, S.J.R. Simons, C.D. Hills, P.J. Carey, A review of accelerated carbonation technology in the treatment of cement-based materials and sequestration of CO_2, J. Hazard Mater. 112 (2004) 193–205.
[119] C.F. Liang, B.L. Li, M.Z. Guo, S.D. Hou, S.X. Wang, Y.Q. Gao, X.Y. Wang, Effects of early-age carbonation curing on the properties of cement-based materials: a review, J. Build. Eng. 84 (2024) 108495.
[120] L.X. Li, M.Z. Wu, An overview of utilizing CO_2 for accelerated carbonation treatment in the concrete industry, J. CO_2 Util. 60 (2020) 102000.
[121] P. Xia, S. Wang, K. Chen, T. Meng, X. Chen, F. Gong, A recycling approach of natural stone from crushed concrete based on freeze-thaw modification and usage of spalling mortar as recycled fine aggregate, Constr. Build. Mater. 416 (2024) 135287.
[122] X.C. Shi, Z.H. Shui, X.G. Xiao, Use of ultraviolet pretreatment to enhance carbonation properties of fly-ash cement under accelerated carbonation at different CO_2 concentrations, J. Build. Eng. 75 (2023) 106983.
[123] P. Sulapha, S.F. Wong, T.H. Wee, S. Swaddiwudhipong, Carbonation of concrete containing mineral admixtures, J. Mater. Civ. Eng. 15 (2) (2003) 134–143.
[124] W.J.J. Huijgen, R.N.J. Comans, C.O. Mineral, $_2$ sequestration by steel slag carbonation, Environ. Sci. Technol. 39 (24) (2005) 9676–9682.
[125] N.L. Ukwattage, P.G. Ranjith, X. Li, Steel-making slag for mineral sequestration of carbon dioxide by accelerated carbonation, Measurement 97 (2017) 15–22, https://doi.org/10.1016/j.measurement.2016.10.057.
[126] B.B. Guo, G.X. Chu, R.C. Yu, Effects of sufficient carbonation on the strength and microstructure of CO_2-cured concrete, J. Build. Eng. 76 (2023) 107311.
[127] H.M. Zeng, Z.C. Liu, F.Z. Wang, Effect of accelerated carbonation curing on mechanical property and microstructure of high volume steel slag mortar, J. Chin. Ceram. Soc. 48 (2020) 1801–1807, https://doi.org/10.14062/j.issn.0454-5648.20200200 (in Chinese).
[128] D. Zhi, P. Xia, S. Wang, F. Gong, W. Cao, D. Wang, T. Ueda, RBSM-based mesoscale study of mechanical properties and frost damage behaviors for recycled fine aggregate concrete, Constr. Build. Mater. 416 (2024) 135136.
[129] N.L. Ukwattage, P.G. Ranjith, M. Yellishetty, H.H. Bui, T. Xu, A laboratory-scale study of the aqueous mineral carbonation of coal fly ash for CO_2 sequestration, J. Clean. Prod. 103 (2015) 665–674, https://doi.org/10.1016/j, jclepro.2014.03.005.
[130] M. Bauer, N. Gassen, H. Stanjek, S. Peiffer, Carbonation of lignite fly ash at ambient T and P in a semi-dry reaction system for CO_2 sequestration, Appl. Geochem 26 (2011) 1502–1512.
[131] S.J. Gerdemann, W.K. O'Connor, D.C. Dahlin, L.R. Penner, H. Rush, Ex situ aqueous mineral carbonation, Environ. Sci. Technol. 41 (2007) 2587–2593.
[132] B.M. Fernández, S.J.R. Simons, C.D. Hills, P.J. Carey, A review of accelerated carbonation technology in the treatment of cement based materials and sequestration of CO2, J. Hazard Mater. 112 (2004) 193–205.
[133] A. Polettini, R. Pomi, A. Stramazzo, CO_2 sequestration through aqueous accelerated carbonation of BOF slag: a factorial study of parameters effects, J. Environ. Manag 167 (2016) 185–195, https://doi.org/10.1016/j.jenvman.2015.11.042.
[134] L.W. Mo, F. Zhang, D.K. Panesar, M. Deng, Development of low-carbon cementitious materials via carbonating Portland cement-fly ash-magnesia blends under various curing scenarios: a comparative study, J. Clean. Prod. 163 (2017) 252–261.
[135] Z.Y. Liu, P.V.D. Heede, C. Zhang, X.Y. Shi, L. Wang, J. Li, Yan Yao, B. Lothenbach, N.D. Belie, Carbonation of blast furnace slag concrete at different CO_2 concentrations: carbonation rate, phase assemblage, microstructure and thermodynamic modelling, Cem. Concr. Res. 169 (2023) 107161.
[136] D. Cui, W. Sun, N. Banthia, Use of tomography to understand the influence of preconditioning on carbonation tests in cement-based materials, Cem. Concr. Compos 88 (2018) 52–63.
[137] Y.X. Li, X.L. Guo, Coupling evaluation of carbon emissions and strength: early carbonation curing of cement mortar containing incinerated sewage sludge ash (ISSA), Constr. Build. Mater. 427 (2024) 136278.
[138] D.M. Yan, J.Y. Lu, Y.F. Sun, T. Wang, T. Meng, Q. Zeng, Y. Liu, Morphological characteristics of calcium carbonate crystallization in CO_2 pre-cured aerated concrete, RSC Adv. 12 (2022) 14610.
[139] X.Z. Zhong, L.F. Li, Y. Jiang, T.C. Ling, Elucidating the dominant and interaction effects of temperature, CO_2 pressure and carbonation time in carbonating steel slag blocks, Constr. Build. Mater. 302 (2021) 124158.
[140] M.F. Ba, T. Xue, Z.M. He, H. Wang, J.Z. Liu, Carbonation of magnesium oxysulfate cement and its influence on mechanical performance, Constr. Build. Mater. 223 (2019) 1030–1037, https://oi.org/10.1016/j.conbuildmat.2019.07.341.
[141] D.M. Yan, J.Y. Lu, Y.F. Sun, T. Wang, T. Meng, Q. Zeng, Y. Liu, CO_2 Pretreatment to aerated concrete with high-volume industry wastes enables a sustainable precast concrete industry, ACS Sustain Chem. Eng. 9 (2021) 3363–3375.
[142] J. Bawab, H. El-Hassan, A. El-Dieb, Jamal Khatib, Accelerated carbonation curing of concrete incorporating calcium carbide residue, J. Build. Eng. 88 (2024) 109258.
[143] H.T. Liao, Y.T. Ju, H.X. Lyu, T.J. Liu, D.S. Han, Y. Li, Compressive strength development and microstructure evolution of mortars prepared using reactivated cementitious materials under carbonation curing, Dev. Built Environ. 18 (2024) 100397.
[144] P. Shi, H.X. He, G.C. Marano, Improving the carbonation performance of sulfate-activated material cured waste sediments by calcined Mg-Al hydrotalcite: influence of CLDH dosages, carbonation concentrations and cycles, Constr. Build. Mater. 421 (2024) 135604.

[145] M.S.B. Shafique, J.C. Walton, N. Gutierrez, R.W. Smith, A.J. Tarquin, Influence of carbonation on leaching of cementitious wasteforms, J. Environ. Eng. 124 (1998) 463–467.
[146] J. Temuujin, A. Minjigmaa, B. Davaabal, U. Bayarzul, A. Ankhtuya, T. Jadambaa, K.J.D. MacKenzie, Utilization of radioactive high-calcium Mongolian fly ash for the preparation of alkali-activated geopolymers for safe use as construction materials, Ceram. Int. 40 (10) (2014) 16475–16483, https://doi.org/10.1016/j.ceramint.2014.07.157.
[147] T.F. Chen, M.J. Bai, X.J. Gao, Carbonation curing of cement mortars incorporating carbonated fly ash for performance improvement and CO_2 sequestration, J. CO_2 Util. 51 (2021) 101633.
[148] D. Zhang, S.M. ASCE, X.H. Cai, Y.X. Shao, Carbonation curing of precast fly ash concrete, J. Mater. Civ. Eng. 28 (11) (2016) 04016127.
[149] G.S. Li, S.H. Liu, X. Hu, J.P. Zhu, X.M. Guan, C.J. Shi, Effect of different aggregates on the properties of carbonated self-pulverized low-calcium clinker mortar, Constr. Build. Mater. 408 (2023) 133633.
[150] C.J. Shi, Q. Zou, F.Q. He, Study on CO_2 curing kinetics of concrete, J. Chin. Ceram. Soc. 38 (7) (2010) 1179–1184.
[151] Y. Wang, B. Lu, X. Hu, J.H. Liu, Z.H. Zhang, X.Y. Pan, Z.B. Xie, J. Chang, T. T. Zhang, M.L. Nehdi, C.J. Shi, Effect of CO_2 surface treatment on penetrability and microstructure of cement-fly ash–slag ternary concrete, Cem. Concr. Comp. 123 (2021) 104194.
[152] T. Guo, H.F. Wang, H.J. Yang, X.S. Cai, Q. Ma, S.M. Yang, The mechanical properties of magnesium oxysulfate cement enhanced with 517 phase magnesium oxysulfate whiskers, Constr. Build. Mater. 150 (2017) 844–850, https://doi.org/10.1016/j, conbuildmat. 2017.06.024.
[153] P.P. He, C.S. Poon, D.C.W. Tsang, Comparison of glass powder and pulverized fuel ash for improving the water resistance of magnesium oxychloride cement, Cem. Concr. Compos 86 (2017) 98–109.
[154] K. Gu, B. Chen, H.F. Yu, N. Zhang, W.L. Bi, Y. Guan, Characterization of magnesiumcalcium oxysulfate cement prepared by replacing $MgSO_4$ in magnesium oxysulfate cement with untreated desulfurization gypsum, Cem. Concr. Compos 121 (2021) 104091, https://doi.org/10.1016/j.cemconcomp.2021.104091.
[155] L. Qin, X.T. Mao, X.J. Gao, P. Zhang, T.F. Chen, Q.Y. Li, Y.F. Cui, Performance degradation of CO_2 cured cement-coal gangue pastes with low-temperature sulfate solution immersion, Case Stud. Constr. Mat. 17 (2022) e01199.
[156] T.L. Chen, Y.H. Chen, M.Y. Dai, P.C. Chiang, Stabilization-solidification-utilization of MSWI fly ash coupling CO_2 mineralization using a high-gravity rotating packed bed, Waste Manag. 121 (2021) 412–421.
[157] Y. Hu, Q. Huan, J.H. Lai, X.Y. Yao, C.Y. Song, M. Song, Modification of multi-source industrial solid waste with porous materials to produce highly polymerizeosilica gel: microstructure optimization and CO_2 mineralization enhancement mechanism, Sep Purif. Technol. 336 (2024) 126225.
[158] X.Y. Pan, C.J. Shi, N. Farzadnia, X. Hu, J.L. Zheng, Properties and microstructure of CO_2 surface treated cement mortars with subsequent lime-saturated water curing, Cem. Concr. Compos 99 (2019) 89–99.
[159] S. Kashef-Haghighi, Y.X. Shao, S. Ghoshal, Mathematical modeling of CO_2 uptake by concrete during accelerated carbonation curing, Cem. Concr. Res. 67 (2015) 1–10, https://doi.org/10.1016/j.cemconres.2014.07.020.
[160] A.S. Su, T.F. Chen, X.J. Gao, Q.Y. Li, L. Qin, Effect of carbonation curing on durability of cement mortar incorporating carbonated fly ash subjected to Freeze-Thaw and sulfate attack, Constr. Build. Mater. 341 (2022) 127920.
[161] D. Zhang, Y.X. Shao, Effect of early carbonation curing on chloride penetration and weathering carbonation in concrete, Constr. Build. Mater. 123 (2016) 516–526.
[162] V. Rostami, Y.X. Shao, A.J. Boyd, Z. He, Microstructure of cement paste subject to early carbonation curing, Cem. Concr. Res. 42 (1) (2012) 186–193.
[163] B.X. Song, C.J. Shi, X. Hu, K. Ouyang, Y.H. Ding, G.J. Ke, Effect of early CO_2 curing on the chloride transport and binding behaviors of fly ash-blended Portland cement, Constr. Build. Mater. 288 (2021) 123113.
[164] D. Zhang, Z. Ghouleh, Y.X. Shao, Review on carbonation curing of cement-based materials, J. CO_2 Util. 21 (2017) 119–131, https://doi.org/10.1016/j.jcou. . 2017.07.003.
[165] C. Li, J.H. Wan, H.H. Sun, L.T. Li, Investigation on the activation of coal gangue by a new compound method, J. Hazard Mater. 179 (1-3) (2010) 515–520, https://doi.org/10.1016/j.jhazmat.2010.03.033.
[166] L. Qin, X.J. Gao, W.G. Li, H. Ye, Modification of Magnesium Oxysulfate Cement by Incorporating Weak Acids, in: J Mater Civ Eng, 30, 2018, p. 04018209, https://doi.org/10.1061/(ASCE)MT.1943-5533.0002418.
[167] Y.Y. Huang, C. Xu, H.X. Li, Z.W. Jiang, Z.Q. Gong, X.J. Yang, Q. Chen, Utilization of the black tea powder as multifunctional admixture for the hemihydrate gypsum, J. Clean. Prod. 210 (2019) 231–237, https://doi.org/10.1016/j.jclepro.2018.10.304.
[168] I. Sánchez, X.R. Nóvoa, G.D. Vera, M.A. Climent, Microstructural modifications in Portland cement concrete due to forced ionic migration tests. Study by impedance spectroscopy, Cem. Concr. Res. 38 (7) (2008) 1015–1025.
[169] Q.F. Guan, Y.F. Ma, M. Jin, H.Y. Zeng, C. Gao, J.H. Tang, J.Z. Liu, F.Y. Han, W. W. Li, J.P. Liu, Carbonation curing of belite-rich cement: the role of fly ash and strengthening mechanism, Cem. Concr. Comp. 149 (2024) 105530.
[170] B. Lu, S. Drissi, J.H. Liu, X. Hu, B.X. Song, C.J. Shi, Effect of temperature on CO_2 curing, compressive strength and microstructure of cement paste, Cem. Concr. Res. 2022; 157: 106827 106827 (2022), https://doi.org/10.1016/j.cemconres.
[171] D. Sharma, S. Goyal, Accelerated carbonation curing of cement mortars containing cement kiln dust: an effective way of CO_2 sequestration and carbon footprint reduction, J. Clean. Prod. 192 (2018) 844–854, https://doi.org/10.1016/j.jclepro, 2018.05.027.
[172] L. Qin, X.J. Gao, A.S. Su, Q.Y. Li, Effect of carbonation curing on sulfate resistance of cement-coal gangue paste, J. Clean. Prod. 278 (2021) 123897.
[173] J.Z. Xiao, C.H. Wang, T. Ding, A. Akbarnezhad, A recycled aggregate concrete high-rise building: structural performance and embodied carbon footprint, J. Clean. Prod. 199 (2018) 868–881.
[174] Y. Zhao, T.W. Wang, W. Yi, Emergy-accounting-based comparison of carbon emissions of solid waste recycled concrete, Constr. Build. Mater. 387 (2023) 131674.
[175] C. Liu, C. Zhu, G.L. Bai, Z.G. Quan, J. Wu, Experimental investigation on compressive properties and carbon emission assessment of concrete hollow block masonry incorporating recycled concrete aggregates, Appl. Sci. 9 (22) (2019) 4870.
[176] C.L. Wu, C. Zhang, J.W. Li, X.J. Wang, W. Jiang, S.Z. Yang, W.L. Wang, A sustainable low-carbon pervious concrete using modified coal gangue aggregates based on ITZ enhancement, J. Clean. Prod. 377 (2022) 134310.
[177] S.A. Miller, A. Horvath, P.J.M. Monteiro, C.P. Ostertag, Greenhouse gas emissions from concrete can be reduced by using mix proportions, geometric aspects, and age as design factors, Environ. Res. Lett. 10 (2015) 114017.
[178] B. Lei, L.J. Yu, Z.Y. Chen, W.Y. Yang, C. Deng, Z. Tang, carbon emission evaluation of recycled fine aggregate concrete based on life cycle assessment, Sustainability 14 (21) (2022) 14448.
[179] J.Z. Xiao, H.H. Zhang, Y.X. Tang, Q. Deng, D.C. Wang, C.S. Poon, Fully utilizing carbonated recycled aggregates in concrete: Strength, drying shrinkage and carbon emissions analysis, J. Clean. Prod. 377 (2022) 134520.
[180] S.C. Yaragal, B.C. Kumar, C. Jitin, Durability studies on ferrochrome slag as coarse aggregate in sustainable alkali activated slag/fly ash based concretes, Sustain Mater. Technol. 23 (2020) e00137.
[181] J.J. Wang, Y.F. Wang, C.C. Shi, Y.S. Liu, Strength-based life cycle CO2 of fly ash concrete: variation with common mix parameters, Constr. Build. Mater. 411 (2024) 134365.
[182] H. Kaur, N. Kulthaweepisit, T.N.H. Tran, C. Jaturapitakkul, W. Tangchirapat, Investigation of strength and water permeability of sustainable high-performance concrete containing high-volume ground bottom ash blended with fly ash and nano-silica, J. Build. Eng. 90 (2024) 109428.
[183] X.C. Zhu, Y.S. Zhang, Z.Y. Liu, H.X. Qiao, F.K. Ye, Z. Lei, Research on carbon emission reduction of manufactured sand concrete based on compressive strength, Constr. Build. Mater. 403 (2023) 133101.
[184] J. Thorne, D.V. Bompa, M.F. Funari, N. Garcia-Troncoso, Environmental impact evaluation of low-carbon concrete incorporating fly ash and limestone, Clean. Mater. 12 (2024) 100242.
[185] Y.L. Li, X.S. Shi, Y. Feng, Y.P. Su, Y.H. Zhang, Y.H. Pu, Q.Y. Wang, A novel multi-criteria comprehensive evaluation model of fly ash-based geopolymer concrete, Constr. Build. Mater. 396 (2024) 132253.
[186] C.Q. Wang, D.Y. Duan, X. Li, D.S. Bai, Safe and environmentally friendly use of coal gangue in C30 concrete, Sustain Chem. Pharm. 38 (2024) 101502.
[187] L.F. Li, X. Shao, T.C. Ling, Life cycle assessment of coal gangue composite cements: from sole OPC towards low-carbon quaternary binder, J. Clean. Prod. 414 (2023) 137674.